

Generalised Entanglement Entropies from Unit-Invariant Singular Value Decomposition

Paweł Caputa,^{a,b,c} **Abhigyan Saha**,^c **Piotr Sułkowski**^c

^a *The Oscar Klein Centre and Department of Physics, Stockholm University, AlbaNova, 106 91 Stockholm, Sweden*

^b *Yukawa Institute for Theoretical Physics, Kyoto University, Kitashirakawa Oiwakecho, Sakyo-ku, Kyoto 606-8502, Japan*

^c *Faculty of Physics, University of Warsaw, Pasteura 5, 02-093 Warsaw, Poland*

ABSTRACT: We introduce generalisations of von Neumann entanglement entropy that are invariant with respect to certain scale transformations. These constructions are based on Unit-Invariant Singular Value Decomposition (UISVD) with its right-, left-, and bi-invariant incarnations, which itself are variations of the standard Singular Value Decomposition (SVD) that remain invariant under (appropriate set of) diagonal transformations. These measures are naturally defined for non-Hermitian or rectangular operators and remain useful when the input and output spaces possess different dimensions or metric weights. We apply the UISVD entropy and discuss its advantages in the physically interesting framework of Biorthogonal Quantum Mechanics, whose important aspect is indeed the behavior under scale transformations. Further, we illustrate features of UISVD-based entropies in other representative settings, from simple quantum mechanical bipartite states to random matrices relevant to quantum chaos and holography, and in the context of Chern-Simons theory. In all cases, the UISVD yields stable, physically meaningful entropic spectra that are invariant under rescalings and normalisations.

Contents

1	Introduction	2
2	Unit-Invariant Singular Values	4
2.1	Definitions of singular values	4
2.2	Geometric interpretation	8
2.3	Unit-Invariants for two-dimensional spaces	8
2.4	Unit-Invariant singular values for random matrices	8
3	Unit-Invariant entanglement entropies	11
3.1	Review of entanglement entropy	11
3.2	Unit-Invariant entanglement entropies	12
4	Unit-Invariant SVD entropies for transition matrices	14
4.1	Review of pseudo and SVD entropies	15
4.2	Unit-Invariant SVD entropies	16
5	Applications	17
5.1	Unit-Invariant entropies for the Haar ensemble	17
5.2	Unit-Invariant entropies in Chern-Simons theory	18
5.3	UISVD entanglement entropy for Biorthogonal Quantum Mechanics	22
5.3.1	Biorthogonal entanglement entropies	23
5.3.2	UISVD entropies for transition matrices	25
6	Conclusions and outlook	27
A	Technical details on Unit-Invariant Singular Values	28
B	Results from Random Matrix Theory	33
B.1	Derived Lemmas	34
B.2	Proofs of Section 2.4	43

1 Introduction

Quantum entanglement has become one of the most powerful and unifying concepts in modern theoretical physics. It underlies our understanding of correlations and information in quantum many-body systems [1, 2], quantum field theories [3–5], and even quantum gravity [6–8] through holography [9]. Entanglement entropy and its generalisations have emerged as indispensable probes of quantum structure, diagnosing topological order, characterising quantum phases, and encoding the emergence of spacetime geometry [10]. Still, despite its success, quantifying entanglement in general situations, particularly for mixed states, or for open as well as non-Hermitian systems, remains conceptually and technically challenging.

Traditional measures of entanglement rely on the Schmidt or Singular Value Decomposition (SVD) of a pure state or operator in a bipartite Hilbert space $\mathcal{H} = \mathcal{H}_A \otimes \mathcal{H}_B$ (see [11–13] for more on operator entanglement). For pure states, the Schmidt coefficients fully determine the entanglement spectrum and yield Rényi or von Neumann entropies with clear operational meaning. However, when the system evolves non-unitarily, interacts with an environment, or the setup is described by transition rather than density matrices, the conventional SVD-based framework becomes ambiguous. In such cases, even defining an “entropy” that reflects physical, quantum correlations rather than normalisation or scaling artefacts can be subtle.

Related to these challenges, several generalisations of entanglement have recently been proposed, including pseudo-entropy [14, 15], SVD entropy [16], and entropies in time [17–19] among them. These approaches use the singular values of transition matrices or non-Hermitian operators to construct Rényi-type quantities that extend entanglement to post-selected, time-dependent or general open quantum systems. Such ideas and tools already found applications across diverse areas, from dS/CFT correspondence [17, 20, 21], renormalisation [22], topological theories [23, 24] to spectral form factors used to diagnose quantum chaos [25].

However, a fundamental issue persists across all these constructions: the singular values themselves depend on the choice of units and scaling conventions in the subspaces involved. To see the problem concretely, consider even the simplest quantum mechanical example: a two-level system where one rescales the basis states in one subsystem by an arbitrary factor (a trivial change of normalisation or physical units). Although this transformation leaves the physical content unchanged, it modifies the singular values. As a result, the entropy constructed from those singular values varies under a mere redefinition of scale i.e. conventional SVD, while invariant under unitaries, is not invariant under such diagonal rescalings. Consequently, SVD-based entropic measures may conflate genuine quantum correlations with artefacts of normalisation, a subtle but crucial distinction, especially in field-theoretic or non-Hermitian settings where operator norms (choices of inner-products) or couplings carry non-trivial scaling behaviour (see e.g. [26]).

A mathematically rigorous resolution to this problem with SVD was recently provided by Uhlmann [27]. Following earlier works on construction of singular values invariant under more specific rescalings, he introduced the Unit-Invariant Singular Value Decomposition

(UISVD) as a variation of the standard SVD that remains invariant under diagonal (unit) transformations acting on a given operator from both sides. The UISVD produces unit-invariant singular values that eliminate spurious dependencies on scaling conventions. In effect, UISVD isolates the physically meaningful, scale-independent structure of a linear map.

This property makes the UISVD particularly appealing for the above-mentioned physical setups, where operators often connect Hilbert spaces with different metric or normalisation structures present. Indeed, in these contexts, one may start from entanglement and information measures that are invariant under simple changes of physical units, and hope that classifying them will be easier and more robust, similarly to von Neumann entropies for pure states.

In this work, we introduce the UISVD framework into quantum information and field-theoretic contexts, proposing it as a new foundation for unit-invariant measures of entanglement. We construct UISVD-based analogues of von Neumann entropy and demonstrate the variation from familiar SVD-based quantities while removing their dependence on arbitrary scale choices. These measures are naturally defined for non-Hermitian or rectangular operators and remain robust when the input and output spaces possess different dimensions or metric weights. As a proof of concept, we apply UISVD-based entropies to several representative settings, from simple quantum mechanical bipartite mixed states to random matrices relevant to quantum chaos and holography. In all cases, the UISVD yields stable, physically meaningful entropic spectra that are invariant under rescalings and normalisations.

Beyond their practical advantages, our results suggest a deeper conceptual point: UISVD restores a natural physical covariance to operator-based entropies, ensuring that what we quantify as ‘‘entanglement’’ or ‘‘correlation’’ is independent of arbitrary normalisation or choice of units. In this sense, we hope that UISVD may contribute to providing a unifying, invariant language for quantifying quantum correlations in systems where conventional assumptions of unitarity or normalisation fail.

Let us briefly summarise how we construct scale invariant entropy measures. First, following [27], for a matrix A we introduce its left unit-invariant, right unit-invariant, and (full, left and right) bi-unit-invariant singular values, denoted respectively $\sigma_i^L(A), \sigma_i^R(A)$ and $\sigma_i^B(A)$. Scale (or unit) invariance means that they satisfy the relations

$$\sigma_i^L(A) = \sigma_i^L(DAU), \quad \sigma_i^R(A) = \sigma_i^R(UAD'), \quad \sigma_i^B(A) = \sigma_i^B(DAD'), \quad (1.1)$$

where D and D' are complex non-singular diagonal matrices that represent scaling transformations acting on A from left or right, while U is a unitary matrix (so that left- and right-singular values are in addition invariant under unitary transformation on the opposite side). We then consider quantum systems with bipartite Hilbert spaces $\mathcal{H} = \mathcal{H}_A \otimes \mathcal{H}_B$ characterised by reduced density matrix or reduced transition matrix $\rho_A = \text{Tr}_B(\rho)$, obtained by taking partial trace of a density or transition matrix ρ . The systems of our interest involve some natural scaling operations, which amount to rescaling of ρ_A by diagonal matrices D and D' from left or right, or both sides. We then identify corresponding unit-invariant

singular values, which are scale invariant analogously to Eq. (1.1), and introduce associated unit invariant entropy measures. Depending on the system under consideration, such entropies generalise other familiar versions of entanglement entropy, such as ordinary von Neumann entropy, or pseudo entropy and SVD entropy (when ρ is a transition matrix with respect to some pre- or post-selected state). In the rest of the paper we provide details of such constructions, discuss properties of these entropy measures, and illustrate them in several examples.

This paper is organised as follows. In Section 2, we review the construction of left, right, and bi unit-invariant singular values, and provide their geometric interpretation. To build intuition for these invariants, we compute them explicitly for 2×2 matrices. We also analyse their statistical properties for ensembles of random matrices and show that they obey quarter-circle laws. In Section 3, we use these unit-invariant singular values to define new unit-invariant entanglement entropies for reduced density matrices derived from pure states. Section 4 extends this framework to reduced transition matrices, generalising the pseudo-entropy and SVD-based entropies introduced in the literature. In Section 5, we present several applications of these measures, ranging from random pure states and link-complement states in Chern–Simons theory to Biorthogonal Quantum Mechanics (BQM), where we evaluate, test, and compare them for both reduced density matrices and transition matrices. Finally, we conclude in Section 6 and relegate more technical material to two appendices.

2 Unit-Invariant Singular Values

In this section we review the construction of various scaling invariants of matrices discussed in [27]. We call them left unit-invariant, right unit-invariant, and (full) unit-invariant singular values, and denote respectively LUI-, RUI-, and BUI-singular values. These invariants will play the key role in the construction of entropy measures introduced in next sections. In the following subsections we collect definitions of unit-invariant singular values, provide their geometric interpretation, and present explicit results for two-dimensional spaces.

2.1 Definitions of singular values

To start with, we quickly recall that the Singular Value Decomposition (SVD) of a matrix $A \in \mathbb{C}^{m \times n}$ is

$$A = U\Sigma V^\dagger, \quad (2.1)$$

where $U \in \mathbb{C}^{m \times m}$ and $V \in \mathbb{C}^{n \times n}$ are unitary, and $\Sigma \in \mathbb{R}^{m \times n}$ is (rectangular) diagonal with nonnegative entries $\sigma_1 \geq \sigma_2 \geq \dots \geq 0$. $\sigma_i \equiv \sigma_i(A)$ are singular values of A and can be directly obtained using $\sigma_i = \sqrt{\lambda_i}$, where λ_i are the eigenvalues of $A^\dagger A$. They satisfy the property $\sigma_i(A) = \sigma_i(U'AV')$, i.e. they are invariant under multiplication on the left or right by arbitrary unitaries U' and V' .

We now introduce generalisations of this framework following [27].

Left Unit-Invariant (LUI) singular values. Consider a matrix $A \in \mathbb{C}^{m \times n}$. For each row i of A , its Euclidean norm is given by

$$\|A(i, :) \|_2 = \sqrt{\sum_{j=1}^n |A_{ij}|^2}. \quad (2.2)$$

The left diagonal scale function matrix $D^L(A) \in \mathbb{R}_+^{m \times m}$ is defined as

$$D_{ii}^L = \begin{cases} \frac{1}{\|A(i, :) \|_2}, & \text{if } \|A(i, :) \|_2 > 0 \\ 1, & \text{otherwise.} \end{cases} \quad (2.3)$$

First, we define the *balanced matrix* A^L as

$$A^L := D^L A. \quad (2.4)$$

Then, the singular values of A^L , determined by its singular value decomposition and denoted $\sigma(A^L)$, are called the *left unit-invariant singular values* $\sigma^L(A)$ of the original matrix A

$$\sigma^L(A) := \sigma(A^L). \quad (2.5)$$

So we essentially decompose A as

$$A = (D^L)^{-1} A^L = (D^L)^{-1} U_0 \Sigma_0 V_0^\dagger, \quad (2.6)$$

and call it the *left unit-invariant singular value decomposition (LUI SVD)*. The invariants $\sigma_i^L(A)$ lie on the diagonal of diagonal matrix Σ_0 and are non-negative real numbers. These values possess the invariance property

$$\sigma^L(A) = \sigma^L(DAU), \quad (2.7)$$

for any $D \in \mathcal{D}$, where \mathcal{D} is the space of non-singular diagonal matrices, and any $U \in \mathcal{U}$, where \mathcal{U} is the space of unitary matrices. For an explicit proof of this claim see Appendix A.

Right Unit-Invariant (RUI) singular values. Their definition is analogous to the LUI singular values, and simply involves column norms instead of row norms in the right diagonal scale function matrix

$$D_{jj}^R = \begin{cases} \frac{1}{\|A(:, j)\|_2}, & \text{if } \|A(:, j)\|_2 > 0 \\ 1, & \text{otherwise.} \end{cases} \quad (2.8)$$

The *balanced matrix* A^R is then defined by

$$A^R := A D^R. \quad (2.9)$$

The singular values of A^R , denoted $\sigma(A^R)$, are called the *right unit-invariant singular values* $\sigma^R(A)$ of the original matrix A

$$\sigma^R(A) := \sigma(A^R). \quad (2.10)$$

In this case the *right unit-invariant singular value decomposition (RUISVD)* of A reads

$$A = A^R (D^R)^{-1} = U_1 \Sigma_1 V_1^\dagger (D^R)^{-1}. \quad (2.11)$$

The RUI singular values are invariant under multiplication by $D \in \mathcal{D}$ and $U \in \mathcal{U}$ from right and left respectively

$$\sigma^R(A) = \sigma^R(UAD). \quad (2.12)$$

Bi Unit-Invariant (BUI) singular values. It is a bit harder to implement invariance under simultaneous multiplication by diagonal matrices on left and right. Nevertheless, such a construction was provided in [27]. It amounts to determining a pair of *positive diagonal* matrices from A , denoted $D^{B_L}(A)$ and $D^{B_R}(A)$, and then the *balanced matrix*

$$A^B = D^{B_L} A D^{B_R}. \quad (2.13)$$

A simple example of this construction for matrices A of size 2 is given in Appendix A, along with a code to compute these values for any general matrix. In general, the diagonals D^{B_L} and D^{B_R} are constructed so that both the *row* and *column geometric means* of $|A^B|$ are equal to 1, with the geometric mean taken over the *nonzero* entries. Concretely, this means that for every row i and column j which are not identically zero,

$$\prod_{k: A_{ik}^B \neq 0} |A_{ik}^B| = 1, \quad (1 \leq i \leq m), \quad \prod_{k: A_{kj}^B \neq 0} |A_{kj}^B| = 1, \quad (1 \leq j \leq n). \quad (2.14)$$

When zero entries are present, we adopt precisely the scaling in [28, Program II] as mentioned in [27] applied to $|A|$, which yields positive diagonal D^{B_L}, D^{B_R} and a balanced matrix satisfying Eq. (2.14). If A contains an all-zero row or column, these are removed prior to scaling and the corresponding diagonal entries are set to 1 upon re-embedding; the subsequent BUI results then hold verbatim.¹

Now, the singular values of A^B , denoted $\sigma(A^B)$, are called the *bi unit-invariant singular values* $\sigma^B(A)$ of the original matrix A

$$\sigma^B(A) := \sigma(A^B). \quad (2.15)$$

Equivalently, these values arise on the diagonal of the matrix Σ upon the *bi unit-invariant singular value decomposition (BUISVD)*

$$A = (D^{B_L})^{-1} A^B (D^{B_R})^{-1} = (D^{B_L})^{-1} U_2 \Sigma_2 V_2^\dagger (D^{B_R})^{-1}. \quad (2.16)$$

These BUI singular values possess the invariance property

$$\sigma^B(A) = \sigma^B(DAD'), \quad (2.17)$$

for any $D, D' \in \mathcal{D}$, where again \mathcal{D} is the space of complex non-singular diagonal matrices.

¹See [27, Thm. IV.2, Lem. IV.3, Thm. IV.4, and Appendix C]

Although we do not use it in this paper, for the sake of completion we note that when the matrix $A \in \mathbb{C}^{n \times n}$ is square, there is one more invariant that can be extracted from this construction, namely the *scale-invariant eigenvalues*² of a matrix A

$$\lambda^S(A) := \lambda(A^B). \quad (2.18)$$

This then satisfies the more restricted invariance property

$$\lambda^S(A) = \lambda^S(D_1 A D_2) \quad \forall D_1, D_2 \in \mathcal{D} \quad \text{s.t. } (D_1 D_2) \in \mathbb{R}_{>0}^{n \times n}. \quad (2.19)$$

Several kinds of transformations fall under this category, for example invariance under DAD or DAD^{-1} where $D \in \mathcal{D}$ is any complex non singular diagonal matrix. Of course the case of *positive scalings*, i.e. D_1, D_2 positive real diagonal, automatically satisfies Eq. (2.19).

Normalisation. Recall that the *sum of squares of the singular values* of any matrix is equal to its *Frobenius norm* (Hilbert-Schmidt norm) squared. Specifically, for A^L we get

$$\|A^L\|_F^2 = \sum_{i=1}^{d_A} \sum_{j=1}^{d_B} |A_{ij}^L|^2 = \sum_{k=1}^{\min(d_A, d_B)} (\sigma_k(A^L))^2 = \sum_{k=1}^{\min(d_A, d_B)} (\sigma_k^L(A))^2, \quad (2.20)$$

where d_A and d_B are the numbers of non-zero rows and columns respectively (if A is a matrix with *full support* then $d_A = m, d_B = n$). On the other hand, by construction

$$\|A^L\|_F^2 = \sum_{i=1}^{d_A} \|A^L(i, :) \|_2^2 = \sum_{i=1}^{d_A} 1 = d_A. \quad (2.21)$$

Analogous statements hold for A^R . Therefore, by the Frobenius norm identity, we get

$$\sum_i (\sigma_i^L)^2 = d_A, \quad \sum_i (\sigma_i^R)^2 = d_B. \quad (2.22)$$

This allows us to introduce the normalised left- and right-singular values as

$$\hat{\sigma}_k^L := \frac{\sigma_k^L}{\sqrt{d_A}}, \quad \hat{\sigma}_k^R := \frac{\sigma_k^R}{\sqrt{d_B}}. \quad (2.23)$$

Unfortunately, we were not able to derive a simple expression (in terms of d_A and d_B) for the Frobenius norm of A^B so we just write formally the normalised singular values of A^B as

$$\hat{\sigma}_k^B := \frac{\sigma_k^B}{\|A^B\|_F} = \frac{\sigma_k^B}{\sqrt{\sum_i (\sigma_i^B)^2}}. \quad (2.24)$$

These normalised values will appear directly in our definitions of entropies based on the UISVD decompositions.

²We reserve the notation λ^B for a different construction used later.

2.2 Geometric interpretation

It is worth invoking a geometric interpretation of the quantities introduced above. SVD has a well known representation in Euclidean space: it takes the unit sphere in the input space and turns it into an ellipsoid in the output space. The right singular vectors are the input directions that land on the ellipsoid's principal axes, the left singular vectors point along those axes in the output space, and the singular values are the axis lengths.

LUI-SVD and RUI-SVD keep this same sphere to ellipsoid story, but they first “re-unit” one side by a diagonal stretch of the coordinate axes chosen from the Euclidean row or column norms. In LUI-SVD one stretches or shrinks the output coordinate axes so the nonzero rows have equal size under that norm, which puts the output channels on a common scale before looking for the ellipsoid's principal directions. In RUI-SVD one does the analogous axis rescaling on the input side so the nonzero columns have equal size, which makes the input coordinates comparable before looking for principal directions. After this one-sided axis standardisation, an ordinary SVD gives the ellipsoid geometry in the standardised coordinates, and the diagonal factor just converts that geometric description back to the original units.

BUI-SVD is the fully symmetric version. It diagonally stretches or shrinks both input and output axes until the matrix is balanced in a multiplicative sense, so the products of the nonzero entry magnitudes are equal across nonzero rows and columns, which one can think of as balancing typical entry magnitudes across rows and columns, or as centering log-magnitudes when no zeros are present. Once that balancing has fixed the arbitrary choice of units on both sides, SVD again reads off the same sphere to ellipsoid geometry, now in the balanced coordinate system, and the outer diagonal factors simply map the picture back to the original coordinates.

2.3 Unit-Invariants for two-dimensional spaces

As the simplest illustration, in Table 1 we provide the explicit form of the above invariants (for completeness, also including eigenvalues and singular values) for an arbitrary complex matrix of size 2 with non-zero entries

$$A = \begin{pmatrix} a_1 & a_2 \\ a_3 & a_4 \end{pmatrix}. \quad (2.25)$$

These invariants and their properties are derived in Appendix A.

2.4 Unit-Invariant singular values for random matrices

For completeness and to gain more insight into scale invariance, in this section we investigate distributions of invariants for random matrices drawn from several standard ensembles (Ginibre and Wigner). Our main result is the statement that distributions of these invariants take form of quarter-circle law. To start with, for a fixed dimension n and m independent random matrices, we compute eigenvalues, singular values, as well as left-, right-, and full unit-invariant singular values. We denote them by $\sigma_i^{(j)}$, where $i = 1, \dots, n$

Invariant	Formula
Eigenvalues λ_{\pm}	$\frac{1}{2} \left(a_1 + a_4 \pm \left((a_1 - a_4)^2 + 4a_2a_3 \right)^{\frac{1}{2}} \right)$
Singular values σ_{\pm}	$\left(\frac{1}{2} \left(\sum_{i=1}^4 a_i ^2 \pm \left(\left(\sum_{i=1}^4 a_i ^2 \right)^2 - 4\tilde{a} \right)^{\frac{1}{2}} \right) \right)^{\frac{1}{2}}$
BUI-singular values σ_{\pm}^B	$\left(\hat{a} + \hat{a}^{-1} \pm \left[(\hat{a} + \hat{a}^{-1})^2 - \frac{\tilde{a}}{ a_1a_2a_3a_4 } \right]^{\frac{1}{2}} \right)^{\frac{1}{2}}$
LUI-singular values σ_{\pm}^L	$\left(1 \pm \left(1 - \frac{\tilde{a}}{(a_1 ^2 + a_2 ^2)(a_3 ^2 + a_4 ^2)} \right)^{\frac{1}{2}} \right)^{\frac{1}{2}}$
RUI-singular values σ_{\pm}^R	$\left(1 \pm \left(1 - \frac{\tilde{a}}{(a_1 ^2 + a_3 ^2)(a_2 ^2 + a_4 ^2)} \right)^{\frac{1}{2}} \right)^{\frac{1}{2}}$

Table 1: Closed form expressions for eigenvalues, singular values, and unit-invariant singular values of matrices (2.25) of size 2. Here $\hat{a} := |(a_1a_4)/(a_2a_3)|^{\frac{1}{2}}$ and $\tilde{a} := |a_1a_4 - a_2a_3|^2$.

labels invariants for a given matrix and $j = 1, \dots, m$ labels matrices in a given random set. The empirical spectral measure is

$$\rho(x) = \frac{1}{mn} \sum_{j=1}^m \sum_{i=1}^n \delta(x - \sigma_i^{(j)}), \quad (2.26)$$

estimated by pooling all $m \times n$ samples into a normalised histogram.

Ensemble	β	Construction
Real Ginibre	1	$A = \frac{1}{\sqrt{n}} G, \quad G_{ij} \stackrel{\text{i.i.d.}}{\sim} \mathcal{N}(0, 1)$
Complex Ginibre	2	$A = \frac{1}{\sqrt{n}} G, \quad G_{ij} \stackrel{\text{i.i.d.}}{\sim} \mathcal{CN}(0, 1)$

Table 2: Ginibre β -ensembles.

In Table 2 we present the Ginibre β -ensembles which are constructed using Gaussian entries. In Theorems 2.1 and 2.2 we prove the distribution limits more generally for i.i.d. sub-Gaussian entries, hence the limiting behaviour for the real and complex Ginibre cases ($\beta = 1, 2$) are direct corollaries.

Let $X_n = (X_{ij})_{1 \leq i, j \leq n}$ have i.i.d. entries with mean 0, variance 1, sub-Gaussian tails, $\mathbb{P}(X_{ij} = 0) = 0$, and assume a small-ball bound near 0.³ Consider

$$A_n := \frac{1}{\sqrt{n}} X_n. \quad (2.27)$$

³There exist $\alpha > 0$ and $C_0 < \infty$ such that $\mathbb{P}(|X_{ij}| \leq t) \leq C_0 t^\alpha$ for all $t \in (0, 1)$.

We compute the empirical singular-value measures of A_n^L , A_n^R , and A_n^B which by definition correspond to the empirical measures associated to $\sigma^L(A_n)$, $\sigma^R(A_n)$, and $\sigma^B(A_n)$ respectively.⁴

Theorem 2.1 (Quarter-circle law for LUI- and RUI-SVD). *The empirical singular-value measures of A_n^L and A_n^R converge almost surely to the quarter-circle law on $[0, 2]$ with density $f(s) = \frac{1}{\pi} \sqrt{4 - s^2} \mathbf{1}_{[0,2]}(s)$.*

Proof. See Appendix B.2. □

Theorem 2.2 (Stretched quarter-circle law for BUI-SVD). *Set $c_\star := \mathbb{E} \log |X_{11}| \in \mathbb{R}$. Then, on the unnormalised scale, $\|A_n^B\|_{\mathcal{O}} = 2e^{-c_\star} \sqrt{n} (1+o(1))$ almost surely. The empirical singular-value measures of $T_n := n^{-1/2} A_n^B$ converge to the quarter-circle law on $[0, 2e^{-c_\star}]$ with density $f_\star(s) = \frac{1}{\pi e^{-2c_\star}} \sqrt{(2e^{-c_\star})^2 - s^2} \mathbf{1}_{[0, 2e^{-c_\star}]}(s)$.*

Proof. See Appendix B.2. □

For the special case of Ginibre β -ensembles as in Table 2 we take $X_{ij} = G_{ij}$ choice of Gaussian entries with $c_\star = c_\beta$ for the appropriate entry law.⁵

Ensemble	β	Symmetry	Construction
GOE	1	real symmetric	$G_{ij} \stackrel{iid}{\sim} \mathcal{N}(0, 1)$, $A = \frac{G + G^\top}{\sqrt{2n}}$
GUE	2	complex Hermitian	$G_{ij} \stackrel{iid}{\sim} \mathcal{CN}(0, 1)$, $A = \frac{G + G^\dagger}{\sqrt{2n}}$

Table 3: Wigner β -ensembles.

We also look at Wigner- β ensembles as given in Table 3, and the densities are plotted in Fig. 1 using a large number of matrices.

Theorem 2.3. *Let A_n be GOE/GUE with the $1/\sqrt{n}$ scaling as declared in Table 3. Then the empirical singular-value measures of A_n^L and A_n^R converge almost surely to the quarter-circle law on $[0, 2]$.*

Proof. See Appendix B.2. □

Theorem 2.4. *Let A_n be GOE/GUE with the $1/\sqrt{n}$ scaling. Then $\|A_n^B\|_{\mathcal{O}} = 2e^{-c_\beta} \sqrt{n} (1+o(1))$ almost surely. Equivalently, the singular values of $T_n := n^{-1/2} A_n^B$ converge almost surely to the quarter-circle law on $[0, 2e^{-c_\beta}]$.*

Proof. See Appendix B.2. □

⁴To construct A_n^B we choose the symmetric scale as per Proposition B.10 to fix a unique choice.

⁵The numerical values of c_β are given in Lemma B.12.

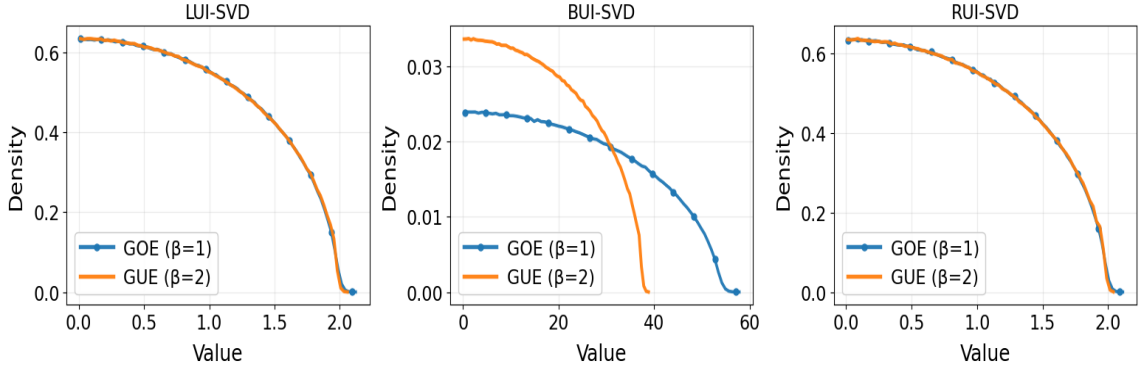


Figure 1: Empirical densities for the invariants $\{\sigma_k^L\}$, $\{\sigma_k^R\}$, and $\{\sigma_k^B\}$ with $n = 200$. LUI and RUI follow the quarter-circle law of singular value distribution. BUI has dimension dependent stretched supports $\approx [0, 2.67\sqrt{n}]$ for GUE, and $\approx [0, 3.77\sqrt{n}]$ for GOE.

3 Unit-Invariant entanglement entropies

In this section we introduce various entanglement entropies based on unit-invariant singular values defined above. They generalise von Neumann, pseudo- or SVD entropies considered earlier in literature, whose definitions and properties we briefly summarise first.

3.1 Review of entanglement entropy

We start with the usual setup of a bipartite Hilbert space

$$\mathcal{H} = \mathcal{H}_{\mathbb{A}} \otimes \mathcal{H}_{\mathbb{B}}, \quad (3.1)$$

with subsystems of arbitrary finite dimensions $d_{\mathbb{A}}$ and $d_{\mathbb{B}}$ respectively. We consider bipartite pure state $|\psi\rangle$ and corresponding density matrix expressed in some fixed orthonormal basis as

$$|\psi\rangle = \sum_{i,k} A_{ik} |i\rangle_{\mathbb{A}} |k\rangle_{\mathbb{B}}, \quad \rho = |\psi\rangle \langle \psi| = \sum_{i,j,k,l} A_{ik} A_{jl}^* |i\rangle_{\mathbb{A}} \otimes |k\rangle_{\mathbb{B}} \langle l|_{\mathbb{B}} \otimes \langle j|_{\mathbb{A}}, \quad (3.2)$$

with coefficient matrix A that does not have any all-zero rows or all-zero columns. The reduced density matrix of \mathbb{A} becomes

$$\rho_{\mathbb{A}} = \text{Tr}_{\mathbb{B}}(\rho) = \sum_{i,j} (AA^\dagger)_{ij} |i\rangle_{\mathbb{A}} \langle j|_{\mathbb{A}}. \quad (3.3)$$

To compute entropies we will consider normalised density matrix $\text{Tr}(\rho_A) = 1$ that we can write as operator⁶

$$\rho_{\mathbb{A}} = \frac{AA^\dagger}{\text{Tr}(AA^\dagger)}. \quad (3.4)$$

⁶It is usually more natural to start this construction with normalising $|\psi\rangle$ so that $\text{Tr}(A^\dagger A) = 1$, but we keep this discussion more general for later purposes.

Then, in the standard computation of von Neumann entropy, we perform the singular value decomposition of A

$$A = U\Sigma V^\dagger, \quad (3.5)$$

with unitaries U and V^\dagger and diagonal matrix Σ with singular values σ_i

$$\Sigma = \text{diag}(\sigma_1, \sigma_2, \dots), \quad (3.6)$$

that leads to

$$\rho_{\mathbb{A}} = \frac{U\Sigma^2 U^\dagger}{\text{Tr}(U\Sigma^2 U^\dagger)} = \frac{U\Sigma^2 U^\dagger}{\text{Tr}(\Sigma^2)}. \quad (3.7)$$

This way, the normalised eigenvalues λ_k of $\rho_{\mathbb{A}}$ are squares of the singular values of A $\lambda_k = \sigma_k^2 / (\sum_l \sigma_l^2)$. Recall that this procedure is equivalent to introducing a *particular basis* in the Hilbert space $\mathcal{H}_{\mathbb{A}} \otimes \mathcal{H}_{\mathbb{B}}$ through the Schmidt decomposition of $|\psi\rangle$ (often understood as a purification of $\rho_{\mathbb{A}}$). Indeed, we can write the state $|\psi\rangle$ using the SVD decomposition (3.5)

$$|\psi\rangle = \sum_{i,j} A_{ij} |i\rangle_{\mathbb{A}} |j\rangle_{\mathbb{B}} = \sum_{i,k,j} U_{ik} \Sigma_{kk} V_{kj}^\dagger |i\rangle_{\mathbb{A}} |j\rangle_{\mathbb{B}} \equiv \sum_k \sigma_k |k\rangle_{\mathbb{A}} |k\rangle_{\mathbb{B}}, \quad (3.8)$$

where we defined the basis vectors

$$|k\rangle_{\mathbb{A}} = \sum_i U_{ik} |i\rangle_{\mathbb{A}}, \quad |k\rangle_{\mathbb{B}} = \sum_j V_{kj}^\dagger |j\rangle_{\mathbb{B}}, \quad (3.9)$$

that span the basis in \mathbb{A} (and its complement \mathbb{B}), and the singular values are also called the Schmidt coefficients.

Finally, from the singular values (Schmidt coefficients), we can evaluate a family of Rényi entropies indexed by an integer n as

$$S_{\mathbb{A}}^{(n)} = \frac{1}{1-n} \log(\text{Tr}(\rho_{\mathbb{A}}^n)) = \frac{1}{1-n} \log \left(\sum_k \lambda_k^n \right) = \frac{1}{1-n} \log \left(\sum_k \frac{(\sigma_k^2)^n}{(\sum_l \sigma_l^2)^n} \right). \quad (3.10)$$

The entanglement (von Neumann) entropy, which can also be obtained as the limit of $n \rightarrow 1$ of the Rényi family, is defined as

$$S_{\mathbb{A}}^{\text{E}} := -\text{Tr}(\rho_{\mathbb{A}} \log(\rho_{\mathbb{A}})) = -\sum_k \lambda_k \log(\lambda_k) = -\sum_k \frac{\sigma_k^2}{(\sum_l \sigma_l^2)} \log \left(\frac{\sigma_k^2}{(\sum_l \sigma_l^2)} \right). \quad (3.11)$$

In what follows we generalise this construction to other decompositions of matrix A discussed in the previous sections.

3.2 Unit-Invariant entanglement entropies

To start with, we consider scale invariant generalisations of von Neumann entropy. We describe three distinct prescriptions by which a *balanced state* associated to (3.2) is defined. Next, we evaluate reduced density matrices $\rho_{\mathbb{A}}$ and entanglement entropies expressed by appropriate normalised singular values.

Left-UI entanglement entropy. We first define the balanced state associated to (3.2) by acting with some diagonal, local⁷ rescaling operator L^ψ on basis vectors in $\mathcal{H}_\mathbb{A}$

$$|\psi^L\rangle := \left[L_\mathbb{A}^\psi \otimes \mathbb{I}_\mathbb{B} \right] |\psi\rangle, \quad L_\mathbb{A}^\psi = \frac{D^L}{\sqrt{d_\mathbb{A}}}. \quad (3.12)$$

More explicitly, we have

$$|\psi^L\rangle = \frac{1}{\sqrt{d_\mathbb{A}}} \sum_{ij} (A)_{ij} D_{ii}^L |i\rangle_\mathbb{A} \otimes |j\rangle_\mathbb{B} = \frac{1}{\sqrt{d_\mathbb{A}}} \sum_{ij} (D^L A)_{ij} |i\rangle_\mathbb{A} \otimes |j\rangle_\mathbb{B}. \quad (3.13)$$

Using the definition of the balanced matrix in Eq. (2.4), we can write this as

$$|\psi^L\rangle = \frac{1}{\sqrt{d_\mathbb{A}}} \sum_{ij} (A^L)_{ij} |i\rangle_\mathbb{A} \otimes |j\rangle_\mathbb{B} = \frac{1}{\sqrt{d_\mathbb{A}}} \sum_k \sigma_k^L |k\rangle_\mathbb{A} \otimes |k\rangle_\mathbb{B}, \quad (3.14)$$

where in the second step we defined the Schmidt vectors (suppressing superscripts of L to ease the notation)

$$|k\rangle_\mathbb{A} = \sum_i (U_0)_{ik} |i\rangle_\mathbb{A}, \quad |k\rangle_\mathbb{B} = \sum_j (V_0^\dagger)_{kj} |j\rangle_\mathbb{B}. \quad (3.15)$$

Since the normalised left singular values are simply $\hat{\sigma}_k^L = \sigma_k^L / \sqrt{d_\mathbb{A}}$, we have the Schmidt decomposition

$$|\psi^L\rangle = \sum_k \hat{\sigma}_k^L |k\rangle_\mathbb{A} \otimes |k\rangle_\mathbb{B}, \quad (3.16)$$

that allows us to define the reduced density matrix of \mathbb{A} evaluated from $|\psi^L\rangle$ as

$$\rho_\mathbb{A}^L = \text{Tr}_\mathbb{B}(|\psi^L\rangle \langle \psi^L|) = \sum_k \left(\hat{\sigma}_k^L \right)^2 |k\rangle_\mathbb{A} \langle k|_\mathbb{A}. \quad (3.17)$$

Finally, we define *Left-Unit-Invariant entanglement entropy* (LUI entanglement entropy) $S_\mathbb{A}^L$ of $\rho_\mathbb{A}$ as the *von Neumann entropy* of $\rho_\mathbb{A}^L$

$$S_\mathbb{A}^L(\rho_\mathbb{A}) := -\text{Tr}(\rho_\mathbb{A}^L \log(\rho_\mathbb{A}^L)) = -\sum_k (\hat{\sigma}_k^L)^2 \log[(\hat{\sigma}_k^L)^2]. \quad (3.18)$$

From the Schmidt decomposition in (3.16), we can easily see that $S_\mathbb{A}^L = S_\mathbb{B}^L$ where $\rho_\mathbb{B}^L = \text{Tr}_\mathbb{A}(|\psi^L\rangle \langle \psi^L|)$. Moreover, by construction, LUI entanglement entropy is invariant under the action on the state $|\psi\rangle$ with any *local, diagonal scaling operator* $D_\mathbb{A}$ on $\mathcal{H}_\mathbb{A}$, and any *local unitary operator* $U_\mathbb{B}$ on $\mathcal{H}_\mathbb{B}$, i.e. it is the same for $|\psi\rangle$ and $|\tilde{\psi}\rangle = D_\mathbb{A} \otimes U_\mathbb{B} |\psi\rangle$.

Right-UI entanglement entropy. In complete analogy to LUI above, we define

$$|\psi^R\rangle := \left[\mathbb{I}_\mathbb{A} \otimes R_\mathbb{B}^\psi \right] |\psi\rangle, \quad R_\mathbb{B}^\psi = \frac{D^R}{\sqrt{d_\mathbb{B}}}, \quad (3.19)$$

⁷Note that we admit different rescalings for each basis vector.

or explicitly

$$|\psi^R\rangle = \frac{1}{\sqrt{d_B}} \sum_{ij} (A^R)_{ij} |i\rangle_A \otimes |j\rangle_B = \frac{1}{\sqrt{d_B}} \sum_k \sigma_k^R |k\rangle_A \otimes |k\rangle_B, \quad (3.20)$$

where we again defined the Schmidt vectors $|k\rangle$ from the SVD decomposition of A^R in Eq. (2.9). The reduced density matrix of \mathbb{B} computed from this state becomes

$$\rho_B^R = \text{Tr}_A(|\psi^R\rangle \langle \psi^R|) = \sum_k (\hat{\sigma}_k^R)^2 |k\rangle_B \langle k|_B, \quad (3.21)$$

and we define the *Right-Unit-Invariant entanglement entropy* (RUI entanglement entropy) S_B^R of ρ_B^R as the von Neumann entropy of ρ_B^R

$$S_B^R(\rho_B^R) := -\text{Tr}(\rho_B^R \log(\rho_B^R)) = -\sum_k (\hat{\sigma}_k^R)^2 \log[(\hat{\sigma}_k^R)^2]. \quad (3.22)$$

Again, the Schmidt decomposition of $|\psi^R\rangle$ in (3.20) implies $S_B^R = S_A^R$ for the entropy of \mathbb{A} computed for $\rho_A^R = \text{Tr}_B(|\psi^R\rangle \langle \psi^R|)$. Also, by construction, RUI entanglement entropy is invariant under the action of $U_A \otimes D_B$ on state $|\psi\rangle$, i.e. it is the same for a family of states $|\tilde{\psi}\rangle = U_A \otimes D_B |\psi\rangle$ with arbitrary unitary in \mathbb{A} and diagonal in \mathbb{B} .

Bi-UI entanglement entropy. Ultimately, we define Bi-Unit-Invariant (BUI) entanglement entropy, taking advantage of the full left- and right-scaling invariants introduced in [27]. To this end we define a balanced state

$$|\psi^B\rangle = \frac{M_A^\psi \otimes N_B^\psi}{\|A^B\|_F} |\psi\rangle, \quad M_A^\psi = D^{B_L}, \quad N_B^\psi = D^{B_R}, \quad (3.23)$$

that can be written explicitly as

$$|\psi^B\rangle = \frac{1}{\|A^B\|_F} \sum_{ij} (D^{B_L} A D^{B_R})_{ij} |i\rangle_A \otimes |j\rangle_B = \sum_k \hat{\sigma}_k^B |k\rangle_A \otimes |k\rangle_B, \quad (3.24)$$

where we used the definition (2.13) and the SVD decomposition of A^B to construct the Schmidt decomposition with its normalised singular values given by Eq. (2.24).

As before, we can evaluate the reduced density matrices ρ_A^B and ρ_B^B by performing partial trace over $\rho^B = |\psi^B\rangle \langle \psi^B|$. Finally, we define the *Bi-Unit-Invariant entanglement entropy* (BUI entanglement entropy) S_A^B of ρ_A^B as the von Neumann entropy of ρ_A^B

$$S_A^B(\rho_A^B) := -\text{Tr}(\rho_A^B \log(\rho_A^B)) = -\sum_k (\hat{\sigma}_k^B)^2 \log[(\hat{\sigma}_k^B)^2]. \quad (3.25)$$

Of course we again have the property $S_A^B = S_B^B$, and this entropy remains invariant under that action on $|\psi\rangle$ with arbitrary diagonal operators of the form $D_A \otimes D_B'$.

4 Unit-Invariant SVD entropies for transition matrices

In turn, motivated by [14, 16], we present a construction involving pre- or post-selected states and scaling invariance of a reduced transition matrix.

4.1 Review of pseudo and SVD entropies

In this case, we generally consider two independent, normalised pure states of the form (3.2) in $\mathcal{H} = \mathcal{H}_{\mathbb{A}} \otimes \mathcal{H}_{\mathbb{B}}$: $|\psi_1\rangle$ and $|\psi_2\rangle$, with non-zero overlap $\langle\psi_2|\psi_1\rangle$. We define the *transition matrix* by

$$\tau^{1|2} = \frac{|\psi_1\rangle\langle\psi_2|}{\langle\psi_2|\psi_1\rangle}, \quad (4.1)$$

which, in general, is a non-Hermitian operator on \mathcal{H} . From this matrix, we compute a partial trace over subsystem \mathbb{B} to obtain the reduced transition matrix operator on \mathbb{A}

$$\tau_{\mathbb{A}}^{1|2} = \text{Tr}_{\mathbb{B}}(\tau^{1|2}). \quad (4.2)$$

Pseudo-entropy [14] is then defined as a generalisation of von Neumann entropy of this transition matrix

$$S_{\mathbb{A}}^P(\tau_{\mathbb{A}}^{1|2}) = -\text{Tr}(\tau_{\mathbb{A}}^{1|2} \log(\tau_{\mathbb{A}}^{1|2})). \quad (4.3)$$

Since the eigenvalues of $\tau_{\mathbb{A}}^{1|2}$ are in general complex, pseudo-entropy will also have real and imaginary parts. These features already found interesting applications in dS/CFT [17], and in holographic CFTs, its gravity dual was found to be the minimal area in Euclidean time-dependent AdS spacetimes [14]. For some specific choices of the pre- and post-selected states, real and imaginary parts of pseudo-entropy were found to satisfy the Kramers–Kronig relations [25]. Nevertheless, the imaginary part of pseudo-entropy makes it hard to interpret it from the quantum information theoretical point of view and its operational meaning remains mysterious. For this reason its “improvement” was proposed in [16] that defined *SVD entropy* as von Neumann entropy computed from the singular values of $\tau_{\mathbb{A}}^{1|2}$, which are real. More precisely, we first construct a density matrix

$$\rho_{\mathbb{A}}^{1|2} = \frac{\sqrt{(\tau_{\mathbb{A}}^{1|2})^\dagger \tau_{\mathbb{A}}^{1|2}}}{\text{Tr} \left[\sqrt{(\tau_{\mathbb{A}}^{1|2})^\dagger \tau_{\mathbb{A}}^{1|2}} \right]}, \quad (4.4)$$

and define the SVD entropy of $\tau_{\mathbb{A}}^{1|2}$ and von Neumann entropy of $\rho_{\mathbb{A}}^{1|2}$

$$S_{\mathbb{A}}^{\text{SVD}}(\tau_{\mathbb{A}}^{1|2}) = -\text{Tr}(\rho_{\mathbb{A}}^{1|2} \log(\rho_{\mathbb{A}}^{1|2})). \quad (4.5)$$

By construction, the singular values σ_k of $\tau_{\mathbb{A}}^{1|2} = U\Sigma V^\dagger$, in $\Sigma = (\sigma_1, \sigma_2, \dots, \sigma_{d_{\mathbb{A}}})$, are related to the normalised eigenvalues $\hat{\lambda}_k$ of $\rho_{\mathbb{A}}^{1|2}$ by

$$\hat{\lambda}_k = \frac{\sigma_k}{\sum_i \sigma_i}, \quad (4.6)$$

so that

$$S_{\mathbb{A}}^{\text{SVD}}(\tau_{\mathbb{A}}^{1|2}) = -\sum_k \hat{\lambda}_k \log(\hat{\lambda}_k). \quad (4.7)$$

By definition, SVD entropy is always non-negative and bounded, $0 \leq S_{\mathbb{A}}^{\text{SVD}} \leq \log(d_{\mathbb{A}})$. Moreover, SVD entropy was given an operational meaning as the average number of Bell pairs distillable from intermediate states that appear between $|\psi_1\rangle$ and $|\psi_2\rangle$ [16]. In the following, we will employ the UISVD values to provide one more generalisation of the pseudo- and SVD entropies.

4.2 Unit-Invariant SVD entropies

Given the above and the UI singular values discussed in Section 2, it is natural to generalise the SVD entropy from Eq. (4.7) by replacing the SVD eigenvalues of $\tau_{\mathbb{A}}^{1|2}$ by its left-, right-, or bi- Unit-Invariant singular values in Eqs. (2.5), (2.10) and (2.15). To proceed systematically, let us first rewrite the transition matrix

$$\tau_{\mathbb{A}}^{1|2} = \sum_{ij} (\tau_{\mathbb{A}}^{1|2})_{ij} |i\rangle_{\mathbb{A}} \langle j|_{\mathbb{A}}, \quad (4.8)$$

as a vector using the Choi–Jamiołkowski isomorphism

$$|\tau_{\mathbb{A}}^{1|2}\rangle = \sum_{ij} (\tau_{\mathbb{A}}^{1|2})_{ij} |i\rangle_{\mathbb{A}} |j\rangle_{\mathbb{A}}^*, \quad (4.9)$$

where $|j\rangle_{\mathbb{A}}^*$ is a CPT conjugate of $|j\rangle_{\mathbb{A}}$. Then we define generalised left-, right-, and bi-UISVD entropies of transition matrix $\tau_{\mathbb{A}}^{1|2}$ as von Neumann entropies computed from singular values of

$$(\tau_{\mathbb{A}}^{1|2})^L = D^L \tau_{\mathbb{A}}^{1|2}, \quad (\tau_{\mathbb{A}}^{1|2})^R = \tau_{\mathbb{A}}^{1|2} D^R, \quad (\tau_{\mathbb{A}}^{1|2})^B = D^{BL} \tau_{\mathbb{A}}^{1|2} D^{BR}, \quad (4.10)$$

where the balanced matrices D^L, D^R and $D^{BL,R}$ are constructed the same way as in Section 2. Note also that, analogously to the UI entropies for states, we can now think about the diagonal scaling operators above as applied to the Choi state in Eq. (4.9).

The SVD values are again computed from

$$(\rho_{\mathbb{A}}^{1|2})^I = \frac{\sqrt{((\tau_{\mathbb{A}}^{1|2})^I)^\dagger (\tau_{\mathbb{A}}^{1|2})^I}}{\text{Tr} \left[\sqrt{((\tau_{\mathbb{A}}^{1|2})^I)^\dagger (\tau_{\mathbb{A}}^{1|2})^I} \right]}, \quad I = L, R, B. \quad (4.11)$$

We denote the UISVD singular values of $(\tau_{\mathbb{A}}^{1|2})^I$ by σ_k^I and the eigenvalues of $(\rho_{\mathbb{A}}^{1|2})^I$ by $\hat{\lambda}_k^I$. They are related by

$$\hat{\lambda}_k^I = \frac{\sigma_k^I}{\sum_i \sigma_i^I}, \quad I = L, R, B. \quad (4.12)$$

Finally, we define the left-, right- or bi- Unit-Invariant SVD entropies of $\tau_{\mathbb{A}}^{1|2}$ as

$$S_{\mathbb{A}}^I(\tau_{\mathbb{A}}^{1|2}) = - \sum_k \hat{\lambda}_k^I \log(\hat{\lambda}_k^I). \quad (4.13)$$

An analogous construction should be performed for $\tau_{\mathbb{B}}^{1|2}$ and, similarly to SVD entropy, in general

$$S_{\mathbb{A}}^I(\tau_{\mathbb{A}}^{1|2}) \neq S_{\mathbb{B}}^I(\tau_{\mathbb{B}}^{1|2}). \quad (4.14)$$

We will study some explicit examples of these quantities in the following sections.

Before we proceed, a few comments are in order. First, let us pick one of the states, say the pre-selected state $|\psi_1\rangle$, and act upon its left or right component with an arbitrary diagonal operator, denoted respectively $D_{\mathbb{A}}$ or $D_{\mathbb{B}}$

$$|\psi_{1\mathbb{A}}\rangle = D_{\mathbb{A}} \otimes \mathbb{I} |\psi_1\rangle \quad \text{and} \quad |\psi_{1\mathbb{B}}\rangle = \mathbb{I} \otimes D_{\mathbb{B}} |\psi_1\rangle. \quad (4.15)$$

The corresponding transition matrices for such rescaled states are then also rescaled by diagonal factors, and we denote them by

$$\tau_{\mathbb{A}}^{1_{\mathbb{A}}|2} = \frac{D_{\mathbb{A}}}{\text{Tr}(D_{\mathbb{A}}\tau_{\mathbb{A}}^{1_{\mathbb{A}}|2})}\tau_{\mathbb{A}}^{1|2} \quad \text{and} \quad \tau_{\mathbb{B}}^{1_{\mathbb{B}}|2} = \frac{D_{\mathbb{B}}}{\text{Tr}(D_{\mathbb{B}}\tau_{\mathbb{B}}^{1_{\mathbb{B}}|2})}\tau_{\mathbb{B}}^{1|2}. \quad (4.16)$$

Thus, for pre-selected states, action of local scaling operators on one of the subsystems and tracing out the complement is equivalent to a scaling of the original transition matrix from the left. Consequently, left- and bi- UISVD entropies will be invariant under such transformations (but R-UISVD will detect them).

Secondly, for the case of post-selected states, any local scaling action results in a scaling on the right

$$\tau_{\mathbb{A}}^{1|2_{\mathbb{A}}} = \tau_{\mathbb{A}}^{1|2} \frac{D_{\mathbb{A}}^{\dagger}}{\text{Tr}(D_{\mathbb{A}}^{\dagger}\tau_{\mathbb{A}}^{1|2})} \quad \text{and} \quad \tau_{\mathbb{B}}^{1|2_{\mathbb{B}}} = \tau_{\mathbb{B}}^{1|2} \frac{D_{\mathbb{B}}^{\dagger}}{\text{Tr}(D_{\mathbb{B}}^{\dagger}\tau_{\mathbb{B}}^{1|2})}. \quad (4.17)$$

Therefore RUISVD and BUISVD entanglement measures would remain invariant, while LUISVD entropy would detect it. Further, acting on the same subsystem of both pre- and post-selected states leads to the two-sided scaling of the original reduced transition matrix, upon which only BUISVD entanglement entropy remains invariant.

In the next section, as a proof of concept, we apply these definitions of unit-invariant entropies to various physical setups.

5 Applications

In this final section we include several natural applications of our UISVD entropies ranging from random states to Chern-Simons theory and Biorthogonal Quantum Mechanics (BQM).

5.1 Unit-Invariant entropies for the Haar ensemble

As the first illustration of the scale-invariant entanglement entropies introduced above, we consider their behaviour for the *Haar ensemble* of bipartite pure states. Let $\mathcal{H} \cong \mathbb{C}^d$ be a finite-dimensional complex Hilbert space with the standard inner product. A random unit vector $|\psi\rangle \in \mathcal{H}$ is called *Haar random* [29–32] if its law is the unique $U(d)$ -invariant probability measure μ_{Haar} on the unit sphere

$$\mathbb{S}(\mathcal{H}) = \{\psi \in \mathcal{H} : \langle \psi | \psi \rangle = 1\}. \quad (5.1)$$

Now specialise to a bipartite Hilbert space

$$\mathcal{H} = \mathcal{H}_{\mathbb{A}} \otimes \mathcal{H}_{\mathbb{B}} \cong \mathbb{C}^{d_{\mathbb{A}}} \otimes \mathbb{C}^{d_{\mathbb{B}}} \cong \mathbb{C}^{d_{\mathbb{A}}d_{\mathbb{B}}}. \quad (5.2)$$

Fix orthonormal product bases $\{|i\rangle\}_{i=1}^{d_{\mathbb{A}}}$ for $\mathcal{H}_{\mathbb{A}}$ and $\{|j\rangle\}_{j=1}^{d_{\mathbb{B}}}$ for $\mathcal{H}_{\mathbb{B}}$. Any pure state $|\psi\rangle \in \mathcal{H}$ can be written as

$$|\psi\rangle = \sum_{i=1}^{d_{\mathbb{A}}} \sum_{j=1}^{d_{\mathbb{B}}} A_{ij} |i\rangle \otimes |j\rangle, \quad (5.3)$$

where $A \in \mathbb{C}^{d_{\mathbb{A}} \times d_{\mathbb{B}}}$ is the *coefficient matrix* of $|\psi\rangle$ in the chosen product basis. In these coordinates, sampling a Haar-random bipartite pure state is equivalent to sampling a random matrix

$$G \in \mathbb{C}^{d_{\mathbb{A}} \times d_{\mathbb{B}}}, \quad G_{ij} \stackrel{\text{i.i.d.}}{\sim} \mathcal{N}(0, 1) + i\mathcal{N}(0, 1), \quad (5.4)$$

and normalising in Hilbert-Schmidt (Frobenius) norm,

$$A = \frac{G}{\sqrt{\text{Tr}(GG^\dagger)}}, \quad (5.5)$$

so that $|\psi\rangle = \text{vec}(A)$ is Haar distributed on $\mathbb{S}(\mathcal{H})$.

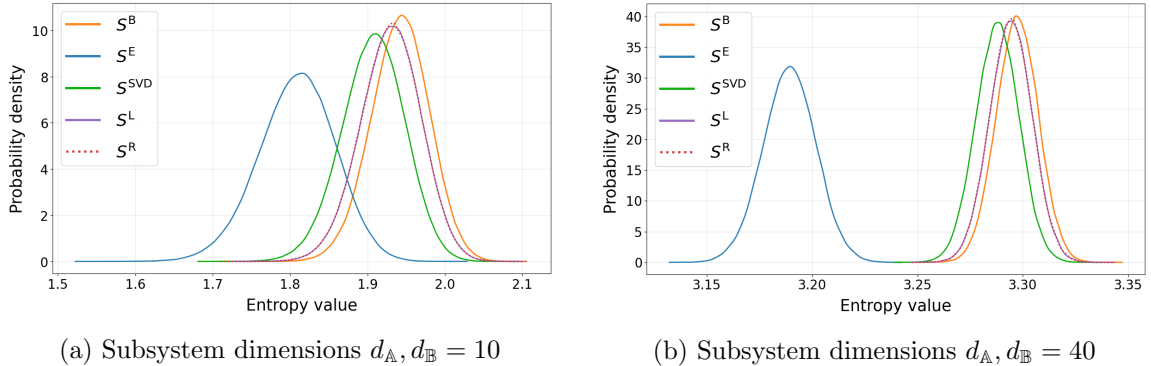


Figure 2: Probability distributions for left-, right- and full unit invariant entanglement entropies S^L, S^R and S^B for Haar ensemble. For completeness we also reproduce the plots of densities of S^E and S^{SVD} from [16]. The *rate of growth with dimension* of all four SVD based entropies is faster than that of the usual entanglement entropy S^E .

We now generate a large ensemble of Haar-random pure states, construct reduced transition matrices $\tau_{\mathbb{A}}^{1|2}$ as in Section 4 using random pairs and, for each, compute left-, right- and bi- Unit-Invariant entanglement entropies S^L, S^R and S^B . For comparison, we also compute the usual bipartite entanglement entropy S^E from each single Haar-random pure state $|\psi\rangle \in \mathcal{H}$ in the ensemble, as well as SVD entropy S^{SVD} , following similar analysis in [16]. Probability distributions for all these measures are shown in Fig. 2. We conclude that scale invariant distributions qualitatively have similar character to the standard ones; they have Gaussian-like shapes, while their averages are shifted towards higher values as

$$S^E < S^{SVD} < S^L \approx S^R < S^B. \quad (5.6)$$

5.2 Unit-Invariant entropies in Chern-Simons theory

As another interesting and illustrative playground, we apply the entanglement measures introduced in Section 3 to Chern-Simons theory, following the line of research that applies and tests ideas from quantum information theory in the realm of Chern-Simons and related systems [24, 33–35]. In particular, in [24], we observed that several entanglement entropy measures defined from transition matrices exhibit intricate connections with link complement states in Chern-Simons gauge theory. Specifically, the imaginary part of pseudo

entanglement entropy S^P , computed from the complex eigenvalues of the reduced transition matrices (4.2), provides a new tool to detect the chirality of the underlying links. This holds for any compact gauge group. For the special case of $U(1)$, it was further shown that the entanglement measure based on the singular values of the reduced transition matrix, called the *excess SVD entanglement entropy* ΔS^{SVD} (constructed using Eq. (4.5)), acts as a *pseudo metric* on the space of two-component links. These observations naturally lead us to ask: what is the physical interpretation (or a useful application) of the entanglement entropies derived from the remaining three invariants discussed in this work, when applied to link complement states?

To this end, consider a two-component link $\mathcal{L} = \mathcal{K}_1 \cup \mathcal{K}_2$ whose link complement state is given by [33, 34]

$$|\mathcal{L}\rangle = \sum_{i,j} V_{ij}^{\mathcal{L}} |i\rangle \otimes |j\rangle, \quad (5.7)$$

where the coefficients $V_{ij}^{\mathcal{L}}$ are *coloured polynomial invariants* (for any gauge group) associated with the link in representations i and j . In the matrix language, we represent these coefficients as the entries of the matrix

$$A = (V_{ij}^{\mathcal{L}}). \quad (5.8)$$

In this setup, we show that the operation of taking the connected sum and a framing change are respectively examples of diagonal and unitary operations, upon which appropriate measures of our interest are invariant (analogously as in Eq. (1.1)).

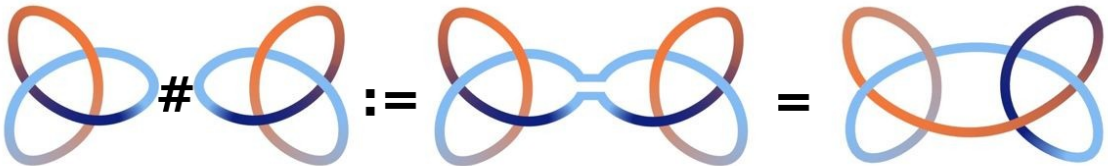


Figure 3: Connected sum of left and right trefoil knots gives a “granny knot”.

We begin with the operation of connected sum. Recall that the *connected sum* $\mathcal{K}\#\mathcal{K}'$ of two knots $\mathcal{K}, \mathcal{K}'$ is defined by first cutting a tiny piece out of each knot so that each one becomes an open string with two loose ends. Then we connect the two knots by joining an end from the first to an end from the second, and joining the remaining two ends, using short connections that don't tangle with anything else. This results in a single closed loop denoted by $\mathcal{K}\#\mathcal{K}'$. An example is shown in Fig. 3 using left and right trefoil knots. Recently, this operation has also found a direct, experimentally realised counterpart in real materials [36].

Suppose given a link $\mathcal{L} = \mathcal{K}_1 \cup \mathcal{K}_2$, we perform a connected sum on the first component with a knot \mathcal{K} and on the second component with a knot \mathcal{K}' , so that we obtain $\mathcal{L}' := (\mathcal{K}\#\mathcal{K}_1) \cup (\mathcal{K}_2\#\mathcal{K}')$. The coloured polynomials (normalised by the unknot) of these knots in representation i and j are given by $V_i^{\mathcal{K}}$ and $V_j^{\mathcal{K}'}$ respectively. We define the corresponding

diagonal operators:

$$D = \text{diag}(V_0^{\mathcal{K}}, V_1^{\mathcal{K}}, V_2^{\mathcal{K}}, \dots) \quad \text{and} \quad D'^{\dagger} = \text{diag}(V_0^{\mathcal{K}'}, V_1^{\mathcal{K}'}, V_2^{\mathcal{K}'}, \dots). \quad (5.9)$$

Equivalently in Eq. (5.9) the matrix D' is constructed out of the coloured polynomial invariants of the *mirror image* of \mathcal{K}' [24]. The action of taking a connected sum on each component is equivalent to applying the local diagonal operator $D \otimes D'$ on the state:

$$(D \otimes D') |\mathcal{L}\rangle = \sum_{i,j} V_i^{\mathcal{K}} V_{ij}^{\mathcal{L}} V_j^{\mathcal{K}'} |i\rangle \otimes |j\rangle. \quad (5.10)$$

Thus, the new quantum state is in the matrix formulation $A' = DAD'$

$$|\mathcal{L}'\rangle = \sum_{i,j} A'_{ij} |i\rangle \otimes |j\rangle = \sum_{i,j} V_i^{\mathcal{K}} V_{ij}^{\mathcal{L}} V_j^{\mathcal{K}'} |i\rangle \otimes |j\rangle = \sum_{i,j} V_{ij}^{\mathcal{L}'} |i\rangle \otimes |j\rangle. \quad (5.11)$$

This shows that connected sum with the knots \mathcal{K} and \mathcal{K}' on the respective components is equivalent to acting on the initial state with the local operator $D \otimes D'$, where each diagonal entry corresponds to the one-coloured polynomial of the knot in that representation. It follows that unit-invariant measures of our interest, which are invariant under diagonal rescalings of this form, are invariant under taking the connected sum.

In turn, we discuss local unitary operations. In the current setup, an interesting class of such operations are changes of *framing* of the component knots. A framing of knot can be interpreted as the linking number of two boundaries of a ribbon created by thickening that knot trajectory. Formally, a framing is a continuous, nowhere-vanishing normal vector field along the knot, effectively turning it into such a twisted ribbon. The *framing number* is the integer that records how many times this field rotates as one traverses the knot once (with the sign determined by the ambient orientation). In our link-complement states, increasing the framing by $+1$ is implemented by a positive *Dehn twist* on the corresponding boundary torus. If we begin with a two-component link with state $|\mathcal{L}\rangle$, and then vary the framing of the first component knot by p and of the second knot by q , then the new link \mathcal{L}' encodes the state [33, 37]

$$|\mathcal{L}'\rangle = \mathcal{T}^p \otimes \mathcal{T}^q |\mathcal{L}\rangle, \quad (5.12)$$

where the Dehn-twist is effected by the matrices \mathcal{T} (e.g. of the form (5.14) in the case $SU(2)$ Chern-Simons theory that we discuss below). These are exactly the relevant local unitary operators that we have been after. In fact, when we are dealing with compact gauge groups, these \mathcal{T} matrices are not just unitary but also diagonal, and a change of framing of each component knot leaves all entropies S^B, S^L, S^R, S^E invariant.

Example. As a concrete example, consider $SU(2)$ Chern-Simons theory at *level* k , in which case the coloured polynomial invariants are the *coloured Jones polynomials*. We consider $\mathcal{L} = 4_1^2$ link, see Fig. 4, which is the simplest example in a family of links denoted $2\mathcal{N}_1^2$, whose coloured Jones polynomials and the associated link complement states take form [33]

$$|2\mathcal{N}_1^2\rangle = \sum_{i,j} \sum_l (\mathcal{S} \mathcal{T}^{\mathcal{N}} \mathcal{S})_{0l} \frac{\mathcal{S}_{il} \mathcal{S}_{jl}}{\mathcal{S}_{0l}} |i\rangle \otimes |j\rangle, \quad i, j \in 0, 1, \dots, k, \quad (5.13)$$

with *modular matrices*

$$\mathcal{T}_{i,j} = e^{\frac{\pi\sqrt{-1}}{4(k+2)} \frac{2i(i+2)-k}{4(k+2)} \delta_{i,j}}, \quad \mathcal{S}_{i,j} = \sqrt{\frac{2}{k+2}} \sin\left(\frac{\pi(i+1)(j+1)}{k+2}\right), \quad (5.14)$$

which satisfy $\mathcal{S}^2 = (\mathcal{S}\mathcal{T})^3 = \mathbb{I}$. For detailed analysis of this family and large k asymptotics of its entanglement entropies see [24]. Now, to either component of this link we connect the trefoil knot 3_1 (again see Fig. 4), whose coloured Jones polynomials are given by [38]

$$V_i^{3_1} = \sum_{l=0}^i (-1)^l q^{\frac{l(l+3)}{2}} (q^{\frac{1}{2}} - q^{-\frac{1}{2}})^{2l} \frac{[i+l+1]!}{[i-l]!}, \quad [x] = \frac{q^{x/2} - q^{-x/2}}{q^{1/2} - q^{-1/2}}, \quad q = e^{\frac{2\pi\sqrt{-1}}{k+2}}. \quad (5.15)$$

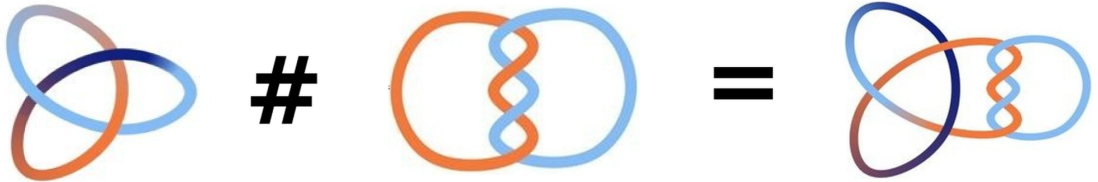


Figure 4: Connected sum of the trefoil knot 3_1 with $2\mathcal{N}_1^2$ link with $\mathcal{N} = 2$, on left side/component resulting in $3_1 \# 4_1^2$.

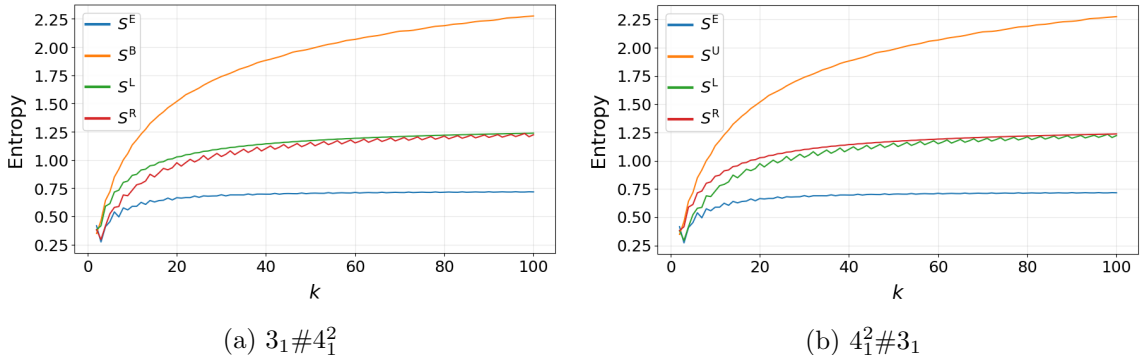


Figure 5: Entanglement entropies S^E, S^B, S^L, S^R versus level k of Chern-Simons.

For this setup, in Fig. 4 we plot various entropy measures of our interest. We observe that S^B curves in both pictures are invariant, which is equal to the S^B of 4_1^2 link complement state, showing invariance under arbitrary connected sum on either component of link. Similarly, the S^L curve of Fig. 5a and S^R curve of Fig. 5b are unaffected by the connected sums on their “own” sides, and is in fact equal to the S^L/S^R of original 4_1^2 (which are equal to each other in that case). However we see that the S^R of Fig. 5a and S^L of Fig. 5b is sensitive to and does indeed detect the connected sum on the “other” side. It was shown in [33] for example that entanglement entropy of $\mathcal{K} \# 2_1^2$ will not distinguish to which

component the knot is connected, but here we see that S^L and S^R do in fact detect the “side” of connected sum in general.

The results in this section hold for any choice of compact gauge group with appropriate choice of coloured polynomials and modular matrices. For example for $SU(N)$ we would use the *coloured HOMFLY-PT polynomials* to construct the link complement states.

5.3 UISVD entanglement entropy for Biorthogonal Quantum Mechanics

Finally, we study the bi-unit-invariant entanglement entropies in another natural setting: Biorthogonal Quantum Mechanics (BQM). BQM is a generalisation of standard quantum mechanics in which scale transformations act as physical symmetries [39]. It is therefore desirable to employ entanglement measures and other observables that remain invariant under such transformations. The unit-invariant measures developed above are ideally suited for this purpose.

We begin by briefly reviewing the essentials of BQM and, in particular, previously studied entanglement measures for biorthogonal states [39], including the standard right–left (RL) construction [40–42]. We then adapt the formalism introduced in the earlier sections to define the BUISVD entanglement entropy in the biorthogonal setting. The key message of this section is that, whereas the conventional RL entanglement entropy is generally complex-valued, may take negative values, and can be unbounded, the BUISVD-based alternative is always real, positive, bounded, and fully compatible with the scaling symmetry of BQM.

Biorthogonal bipartite states. As the name indicates, the defining feature of BQM is a biorthogonal character of its states [39]. We thus consider $\mathcal{H} = \mathcal{H}_{\mathbb{A}} \otimes \mathcal{H}_{\mathbb{B}}$ and fix biorthogonal bases on each factor

$$\{|R_i^{\mathbb{A}}\rangle\}, \{\langle L_i^{\mathbb{A}}|\} \subset \mathcal{H}_{\mathbb{A}}, \quad \{|R_j^{\mathbb{B}}\rangle\}, \{\langle L_j^{\mathbb{B}}|\} \subset \mathcal{H}_{\mathbb{B}}, \quad (5.16)$$

satisfying

$$\langle L_i^{\mathbb{A}} | R_{i'}^{\mathbb{A}} \rangle = \delta_{ii'}, \quad \langle L_j^{\mathbb{B}} | R_{j'}^{\mathbb{B}} \rangle = \delta_{jj'}. \quad (5.17)$$

The corresponding product biorthogonal bases on \mathcal{H} are

$$|R_i^{\mathbb{A}} R_j^{\mathbb{B}}\rangle := |R_i^{\mathbb{A}}\rangle \otimes |R_j^{\mathbb{B}}\rangle, \quad \langle L_i^{\mathbb{A}} L_j^{\mathbb{B}}| := \langle L_i^{\mathbb{A}}| \otimes \langle L_j^{\mathbb{B}}|. \quad (5.18)$$

A biorthogonal state is a pair $(|\Psi_R\rangle, \langle \Psi_L|)$ with expansions

$$|\Psi_R\rangle = \sum_{i,j} \Psi_{ij} |R_i^{\mathbb{A}} R_j^{\mathbb{B}}\rangle, \quad \langle \Psi_L| = \sum_{k,\ell} \Lambda_{k\ell} \langle L_k^{\mathbb{A}} L_\ell^{\mathbb{B}}|, \quad (5.19)$$

subject to the normalisation condition

$$\langle \Psi_L | \Psi_R \rangle = \sum_{i,j} \Lambda_{ij} \Psi_{ij} = 1. \quad (5.20)$$

We collect the right and left coefficients into matrices $\Psi = (\Psi_{ij})$ and $\Lambda = (\Lambda_{ij})$. The admissible BQM scale transformations are rescalings of the biorthogonal bases [26]

$$|R_i^{\mathbb{A}}\rangle \mapsto a_i |R_i^{\mathbb{A}}\rangle, \quad \langle L_i^{\mathbb{A}}| \mapsto a_i^{-1} \langle L_i^{\mathbb{A}}|, \quad |R_j^{\mathbb{B}}\rangle \mapsto b_j |R_j^{\mathbb{B}}\rangle, \quad \langle L_j^{\mathbb{B}}| \mapsto b_j^{-1} \langle L_j^{\mathbb{B}}|, \quad (5.21)$$

with all $a_i, b_j \neq 0$. Under this scaling symmetry the coefficient matrices transform as

$$\Psi_{ij} \mapsto \Psi'_{ij} = a_i^{-1} b_j^{-1} \Psi_{ij}, \quad \Lambda_{ij} \mapsto \Lambda'_{ij} = a_i b_j \Lambda_{ij}, \quad (5.22)$$

i.e.

$$\Psi \mapsto \Psi' = D_{\mathbb{A}}^{-1} \Psi D_{\mathbb{B}}^{-1}, \quad \Lambda \mapsto \Lambda' = D_{\mathbb{A}} \Lambda D_{\mathbb{B}}, \quad (5.23)$$

with $D_{\mathbb{A}} = \text{diag}(a_i)$ and $D_{\mathbb{B}} = \text{diag}(b_j)$.

5.3.1 Biorthogonal entanglement entropies

For a biorthogonal pure state $(|\Psi_R\rangle, \langle \Psi_L|)$ the analogue of a pure-state density operator is [40–42]

$$\rho^{R|L} := |\Psi_R\rangle \langle \Psi_L|, \quad (5.24)$$

which reproduces BQM expectation values via $\langle O \rangle = \text{Tr}(\rho^{R|L} O) / \text{Tr} \rho^{R|L}$ for operator O . From the perspective of our work, we will simply think about it as transition matrix (i.e. weak measurement) and extract its L-, R-, B- singular values the same way as we defined for transition matrices in Section 4. The biorthogonal reduced operator on \mathbb{A} is defined by the partial trace over \mathbb{B} . In product biorthogonal basis

$$\text{Tr}_{\mathbb{B}}(O) = \sum_j \left(I_{\mathbb{A}} \otimes \langle L_{\mathbb{B}}^j | \right) O \left(I_{\mathbb{A}} \otimes | R_{\mathbb{B}}^j \rangle \right). \quad (5.25)$$

Equivalently for matrix elements $(\text{Tr}_{\mathbb{B}} O)_{ik} = \sum_j \langle L_{\mathbb{A}}^i L_{\mathbb{B}}^j | O | R_{\mathbb{A}}^k R_{\mathbb{B}}^j \rangle$. Thus

$$\rho_{\mathbb{A}}^{R|L} := \text{Tr}_{\mathbb{B}} \rho^{R|L} = \sum_{i,j,k} \psi_{ij} \Lambda_{kj} | R_{\mathbb{A}}^k \rangle \langle L_{\mathbb{A}}^i |, \quad (5.26)$$

or in the matrix form $\rho_{\mathbb{A}}^{R|L} = \Psi \Lambda^T$. Under a BQM scale transformation the reduced operator transforms by diagonal similarity

$$\rho_{\mathbb{A}}^{R|L} \mapsto \rho_{\mathbb{A}}^{R|L'} = D_{\mathbb{A}}^{-1} \rho_{\mathbb{A}}^{R|L} D_{\mathbb{A}}, \quad (5.27)$$

so its eigenvalues are invariant under the admissible rescalings.

Let λ_k denote the eigenvalues of $\rho_{\mathbb{A}}^{R|L}$. With the normalisation $\langle \Psi_L | \Psi_R \rangle = 1$ one has $\text{Tr} \rho_{\mathbb{A}}^{R|L} = \sum_k \lambda_k = 1$ but, the same as for transition matrices $\tau_{\mathbb{A}}^{1|2}$, the λ_k 's can be complex because $\rho_{\mathbb{A}}^{R|L}$ is non-Hermitian. The standard “biorthogonal entanglement entropy” used in the BQM literature is the *RL entropy* [40–42]

$$S_{\text{RL}}^E(\Psi) := - \sum_k \lambda_k \log \lambda_k = S_{\mathbb{A}}^P(\rho_{\mathbb{A}}^{R|L}), \quad (5.28)$$

which is simply the pseudo entropy Eq. (4.3) of $\rho_{\mathbb{A}}^{R|L}$. This quantity is scale invariant (it depends only on the spectrum $\{\lambda_k\}$) but generically complex and not bounded by $\log \dim \mathcal{H}_{\mathbb{A}}$. A variant which we denote by $S_{\text{TTC}}^E(\Psi)$ [43, 44], uses the same spectrum $\{\lambda_k\}$ but replaces $\log \lambda_i$ by $\log |\lambda_k|$ in order to remove branch-cut ambiguities while retaining sensitivity to non-Hermiticity. This TTC entropy is again scale invariant but, like S_{RL}^E , is

not a non-negative, bounded entropy. In view of these deficiencies, we now see that the UISVD entanglement measures introduced in this paper may prove to be useful.

UISVD entropy in BQM. We now evaluate the BUISVD entanglement entropy (4.13) directly for the reduced operator $\rho_{\mathbb{A}}^{R|L}$ as

$$S_{\mathbb{A}}^B(\rho_{\mathbb{A}}^{R|L}) = - \sum_k \hat{\sigma}_k^B \log \hat{\sigma}_k^B, \quad \hat{\sigma}_k^B = \frac{\sigma_k^B(\rho_{\mathbb{A}}^{R|L})}{\sum_i \sigma_i^B(\rho_{\mathbb{A}}^{R|L})}, \quad (5.29)$$

where $\hat{\sigma}_k^B$ are bi-unit-invariant singular values (2.15) of $\rho_{\mathbb{A}}^{R|L}$. Since σ_k are non-negative and not all zero, the $\hat{\sigma}_k$ form a bona fide probability vector, so

$$0 \leq S_{\mathbb{A}}^B(\rho_{\mathbb{A}}^{R|L}) \leq \log r, \quad (5.30)$$

where $r = \text{rank } \rho_{\mathbb{A}}^{R|L} \leq \min(\dim \mathcal{H}_{\mathbb{A}}, \dim \mathcal{H}_{\mathbb{B}})$. Moreover, $S_{\mathbb{A}}^B(\rho_{\mathbb{A}}^{R|L})$ is invariant under all admissible BQM rescalings of the biorthogonal bases, in consequence of the invariance of the BUI singular values of $\rho_{\mathbb{A}}^{R|L}$, as seen in Eq. (5.27). This quantity, however, is asymmetric in the indices and depends on the choice of subsystem to be traced out.

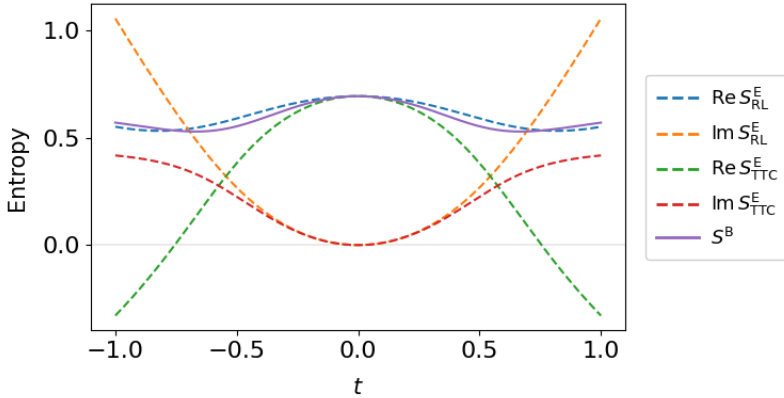


Figure 6: Real and imaginary parts of S_{RL}^E and S_{TTC}^E together with the BUISVD entropy S^B as functions of the parameter t .

Example. To illustrate the difference between S_{RL}^E , S_{TTC}^E , and S^B , consider a two-qubit BQM pure state with a simple analytic dependence on a real parameter t . Take $\dim \mathcal{H}_{\mathbb{A}} = \dim \mathcal{H}_{\mathbb{B}} = 2$ with indices $i, j \in \{0, 1\}$ and product biorthogonal basis $\{|R_i^{\mathbb{A}} R_j^{\mathbb{B}}\rangle\}$ and dual basis $\{ \langle L_i^{\mathbb{A}} L_j^{\mathbb{B}} | \}$. For each real t define the right and left states by

$$|\Psi_R(t)\rangle = |R_0^{\mathbb{A}} R_0^{\mathbb{B}}\rangle + |R_1^{\mathbb{A}} R_1^{\mathbb{B}}\rangle, \quad \langle \Psi_L(t)| = \frac{1}{2} \langle L_0^{\mathbb{A}} L_0^{\mathbb{B}}| - \frac{t}{2} \langle L_0^{\mathbb{A}} L_1^{\mathbb{B}}| + \left(-\frac{t}{2} + it\right) \langle L_1^{\mathbb{A}} L_0^{\mathbb{B}}| + \frac{1}{2} \langle L_1^{\mathbb{A}} L_1^{\mathbb{B}}|, \quad (5.31)$$

so that $\langle \Psi_L(t) | \Psi_R(t) \rangle = 1$ for all t . In the product basis the corresponding coefficient matrices are

$$\Psi = \begin{pmatrix} 1 & 0 \\ 0 & 1 \end{pmatrix}, \quad \Lambda = \frac{1}{2} \begin{pmatrix} 1 & -t \\ -t + 2it & 1 \end{pmatrix}. \quad (5.32)$$

In fact, any pair of Ψ, Λ which satisfies $\text{Tr}(\Lambda^T \Psi) = 1$ is a valid BQM state. The biorthogonal reduced operator on \mathbb{A} is

$$\rho_{\mathbb{A}}^{\text{R|L}}(t) = \Psi \Lambda^T = \frac{1}{2} \begin{pmatrix} 1 & -t + 2it \\ -t & 1 \end{pmatrix}, \quad (5.33)$$

whose eigenvalues and BUI singular values can be explicitly and directly computed using Table 1 and are used to generate the plots in Fig. 6. These plots explicitly illustrate that BUISVD entropy S^B is real and bounded, contrary to S_{RL}^E and S_{TTC}^E .

5.3.2 UISVD entropies for transition matrices

We now turn to BUISVD entanglement measures for pre/post-selected pairs of biorthogonal states and the actual transition matrices in BQM, following recent work [45, 46] on entropies for transition matrices in non-Hermitian systems [43], and also generalising the approach of Section 4.

Biorthogonal transition operators. On the same bipartite Hilbert space $\mathcal{H} = \mathcal{H}_{\mathbb{A}} \otimes \mathcal{H}_{\mathbb{B}}$ with product biorthogonal bases $\{|R_i^{\mathbb{A}} R_j^{\mathbb{B}}\rangle\}$ and $\{|\langle L_i^{\mathbb{A}} L_j^{\mathbb{B}}|\}$ as before, consider two biorthogonal pure states

$$(|\Psi_R^{(1)}\rangle, \langle \Psi_L^{(1)}|), \quad (|\Psi_R^{(2)}\rangle, \langle \Psi_L^{(2)}|), \quad (5.34)$$

each normalised so that $\langle \Psi_L^{(k)} | \Psi_R^{(k)} \rangle = 1$ for $k = 1, 2$. In the product basis we write

$$|\Psi_R^{(1)}\rangle = \sum_{i,j} \Psi_{ij}^{(1)} |R_i^{\mathbb{A}} R_j^{\mathbb{B}}\rangle, \quad \langle \Psi_L^{(2)}| = \sum_{p,q} \Lambda_{pq}^{(2)} \langle L_p^{\mathbb{A}} L_q^{\mathbb{B}}|, \quad (5.35)$$

with coefficient matrices $\Psi^{(1)} = (\Psi_{ij}^{(1)})$ and $\Lambda^{(2)} = (\Lambda_{pq}^{(2)})$. The corresponding right-left transition matrix is

$$\tau^{1|2} = |\Psi_R^{(1)}\rangle \langle \Psi_L^{(2)}|. \quad (5.36)$$

The reduced transition matrix on \mathbb{A} is defined by the biorthogonal partial trace over \mathbb{B} ,

$$\tau_{\mathbb{A}}^{1|2} = \text{Tr}_{\mathbb{B}}(\tau^{1|2}), \quad (\tau_{\mathbb{A}}^{1|2})_{ip} = \langle L_i^{\mathbb{A}} | \tau_{\mathbb{A}}^{1|2} | R_p^{\mathbb{A}} \rangle = \sum_j \Psi_{ij}^{(1)} \Lambda_{pj}^{(2)}, \quad (5.37)$$

and so as a matrix $\tau_{\mathbb{A}}^{1|2} = \Psi^{(1)}(\Lambda^{(2)})^T$, obtained from the same biorthogonal partial trace rule as in the pure-state case. Under the admissible BQM rescalings the coefficients transform exactly as for a single biorthogonal state. As in the pure-state case, the \mathbb{B} -scale cancels and the surviving \mathbb{A} -scale acts on $\tau_{\mathbb{A}}$ by diagonal similarity, i.e. $\tau_{\mathbb{A}} \mapsto \tau'_{\mathbb{A}} = D_{\mathbb{A}}^{-1} \tau_{\mathbb{A}} D_{\mathbb{A}}$, just like in Eq. (5.27). In particular, the eigenvalues of $\tau_{\mathbb{A}}$ are invariant under all admissible biorthogonal rescalings, and so are BUI-singular values of $\tau_{\mathbb{A}}$.

Pseudo entropy. To compute the pseudo-entropy [14] for the pre/post pair $(|\Psi^{(1)}\rangle, |\Psi^{(2)}\rangle)$ along the bipartition $\mathbb{A}|\mathbb{B}$ in BQM setting [46], we construct the transition-matrix (5.37), and denote the set of its normalised eigenvalues by $\{\hat{\lambda}_k\}$. Then the pseudo entropy is simply given by Eq. (4.3).

Because $\tau_{\mathbb{A}}^{1|2}$ transforms by diagonal similarity, the spectrum $\{\lambda_k\}$ is invariant under all admissible BQM scales and $S_{\mathbb{A}}^P$ is diagonally scale free. However, the eigenvalues λ_k are typically complex and not constrained to lie in $[0, 1]$, so $S_{\mathbb{A}}^P$ is generically complex and its real part is not bounded by $\log \dim \mathcal{H}_{\mathbb{A}}$.

BUISVD entropy. To obtain a real, non-negative, and bounded transition entropy that respects the BQM rescaling symmetry, we replace the eigenvalues by the BUI singular values of $\tau_{\mathbb{A}}$. Let $\sigma_k^B(\tau_{\mathbb{A}}^{1|2})$ denote the BUI singular values of $\tau_{\mathbb{A}}^{1|2}$. These are invariant under arbitrary diagonal left and right scalings. Then we compute the BUISVD entropy Eq. (4.13) in BQM simply using the BUI singular values of $\tau_{\mathbb{A}}^{1|2}$ in Eq. (5.37). By construction $S_{\mathbb{A}}^B(\tau_{\mathbb{A}}^{1|2})$ is invariant under all admissible BQM scales on \mathbb{A} and \mathbb{B} , and satisfies the bounds

$$0 \leq S^B \leq \log r, \quad (5.38)$$

where $r = \text{rank } \tau_{\mathbb{A}} \leq \dim \mathcal{H}_{\mathbb{A}}$. Moreover $S^B = 0$ if and only if $\tau_{\mathbb{A}}^{1|2}$ has rank one. In particular, if the transition operator factorises across the $\mathbb{A}|\mathbb{B}$ with a rank-one factor on \mathbb{A} , then $\tau_{\mathbb{A}}^{1|2}$ has rank one and $S^B = 0$. In this sense S^B is a diagonally scale-free analogue of the SVD-based entropies.

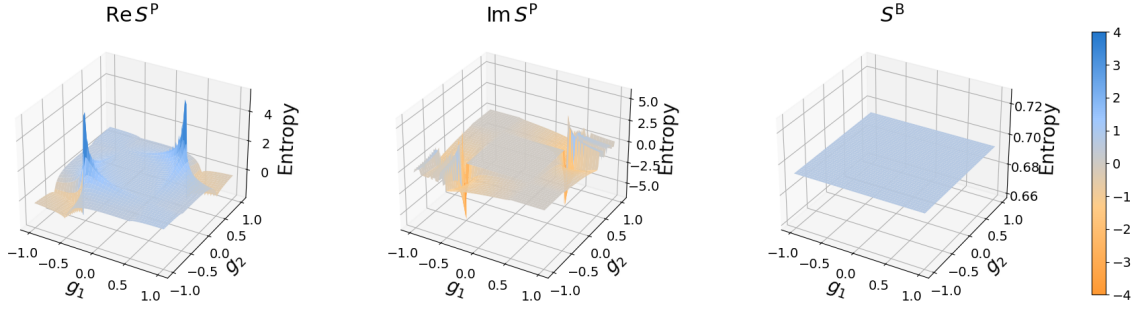


Figure 7: The pre- and post-selected states are taken from the eigenbranch with eigenvalue $E(g) = \sqrt{1 - 4g^2}$ of the two-qubit Hamiltonian, evaluated at g_1 and g_2 respectively. When $g_1 = g_2$ the states are the same, and thus $S^P = S_{\text{RL}}^E$ and BUISVD entropy S^B equals usual BUISVD entropy of state (5.29).

Example. Consider two qubits with Hilbert space $\mathcal{H} = \mathbb{C}^2 \otimes \mathbb{C}^2$, along with Pauli matrices σ^α and define their actions on the two sites by

$$\sigma_1^\alpha = \sigma^\alpha \otimes \mathbb{I}_2, \quad \sigma_2^\alpha = \mathbb{I}_2 \otimes \sigma^\alpha. \quad (5.39)$$

An example of a PT-symmetric non-Hermitian XX Hamiltonian with a staggered imaginary field [47, 48] is

$$H(g) = \sigma_1^x \sigma_2^x + ig(-\sigma_1^z + \sigma_2^z), \quad g \in \mathbb{R} \setminus \{0, \pm \frac{1}{2}\}. \quad (5.40)$$

For each such g we biorthogonally diagonalise $H(g)$

$$H(g) |\Psi_R^{(n)}(g)\rangle = E_n(g) |\Psi_R^{(n)}(g)\rangle, \quad \langle \Psi_L^{(n)}(g) | H(g) = \langle \Psi_L^{(n)}(g) | E_n(g), \quad (5.41)$$

which has the spectrum $E_n(g) \in \{\pm 1, \pm \sqrt{1 - 4g^2}\}$. If we choose any eigenbranch n , then from any two values of g we can obtain two eigenpairs $(|\Psi_R^{(n)}(g_1)\rangle, \langle \Psi_L^{(n)}(g_1)|)$ and $(|\Psi_R^{(n)}(g_2)\rangle, \langle \Psi_L^{(n)}(g_2)|)$, with each eigenpair normalised so that $\langle \Psi_L^{(n)}(g_i)|\Psi_R^{(n)}(g_i)\rangle = 1$. We regard these as the correlated pre- and post-selected BQM states for each pair of g values. With the bipartition $\mathbb{A}|\mathbb{B}$, where \mathbb{A} is the first qubit and \mathbb{B} the second, we form the transition operator

$$\tau^{1|2} = |\Psi_R^{(n)}(g_1)\rangle\langle \Psi_L^{(n)}(g_2)|, \quad (5.42)$$

and its reduced transition matrix $\tau_{\mathbb{A}}^{1|2} = \text{Tr}_{\mathbb{B}}(\tau^{1|2})$. The corresponding pseudo entropy S^P and BUISVD transition entropy S^B are obtained from the eigenvalues and BUI-singular values of $\tau_{\mathbb{A}}^{1|2}$ respectively. Since this $\tau_{\mathbb{A}}^{1|2}$ is a 2×2 matrix, the entropies can be calculated directly using Table 1, and they are plotted in Fig. 7.

6 Conclusions and outlook

The central aim of this work was to introduce unit-invariant singular values into quantum information theory and to use them to define generalised von Neumann-type entropies. After reviewing the basic construction and illustrating it with simple examples, we defined left-, right-, and bi-unit-invariant entanglement entropies for both quantum states and transition matrices. We computed these quantities explicitly and demonstrated their utility across a range of physically diverse and relevant examples, including random matrices, Chern–Simons link-complement states, and Biorthogonal Quantum Mechanics. Our selection of examples was deliberately non-exhaustive and intended primarily as a proof of concept.

We expect these mathematically well-defined tools and entanglement measures to admit many interesting and non-trivial applications in current developments across several areas of physics and mathematics. For instance, there has been significant recent interest in classifying phases and symmetries of general mixed states, notably via SymTFT-based approaches [49]. Since these constructions proceed through purifications and the study of their structural properties, our invariant-based entropies may offer a novel perspective on this problem. Moreover, it will be important to clarify the geometric interpretation of UISVD entropies in the context of (A)dS/CFT. As non-Hermitian quantum mechanics is beginning to play an increasingly prominent role in these settings, we anticipate that UISVD entropies will prove particularly useful there as well, see for example [50]. Further, interesting properties of other types of entropies based on rescaled singular values were discussed e.g. in [51]. On the other hand, various types of singular values underlying our work should be of interest in other contexts in random matrix theory. For example, the normalisations that arise in our diagonal scale functions are similar to those that arise in Sinkhorn algorithm and related bistochastic matrices [52, 53] and deserve further scrutiny.

In many other settings, diagonal rescalings reflect a genuine freedom of units, normalisation, or residual gauge, rather than a numerical artefact. Such scalings appear across a broad range of problems: multi-channel and multiterminal transport and hydrodynamics [54–57], tensor-network and string-net constructions where F -data is defined only up

to gauge choices [58–60], correlator-based spectroscopy where operator normalisations are conventional [61, 62], and calibration problems with per-sensor gain ambiguities [63]. Since the unit-consistent inverse is designed to respect diagonal changes of units, our diagonal-invariant UISVD entropy diagnostics provide a concise, convention-independent way to summarise “spectral” structure in these contexts. We leave analysis of all these ideas for future work.

Acknowledgments

We would like to thank Arindam Bhattacharjee, Nils Carqueville, Giuseppe Di Giulio, Pedram Karimi, Miłosz Panfil, Arani Paul, Souradeep Purkayastha, Pichai Ramadevi, Marko Stošić, Jeffrey Uhlmann, and Karol Życzkowski for useful comments or email conversations. We would also like to thank Anuvab Kayaal for the knot/link graphics. This work was supported by the NCN Sonata Bis 9 grant no. 2019/34/E/ST2/00123 and OPUS grant no. 2022/47/B/ST2/03313 funded by the National Science Center, Poland. PC is supported by the ERC Consolidator grant (number: 101125449/acronym: QComplexity). Views and opinions expressed are however those of the authors only and do not necessarily reflect those of the European Union or the European Research Council. Neither the European Union nor the granting authority can be held responsible for them.

A Technical details on Unit-Invariant Singular Values

In this appendix we collect some explicit results used in computations in the paper. First, we derive unit invariant singular values, and for completeness also eigenvalues and ordinary singular values, for any complex 2×2 matrix

$$A = \begin{pmatrix} a_1 & a_2 \\ a_3 & a_4 \end{pmatrix}, \quad a_i \neq 0. \quad (\text{A.1})$$

Note that for such matrices, the cycle ratio factor equals $\hat{a} := |(a_1a_4)/(a_2a_3)|^{\frac{1}{2}}$ and determinant factor equals $\tilde{a} := |a_1a_4 - a_2a_3|^2$. We will also denote general 2×2 diagonal and unitary matrices by

$$D = \begin{pmatrix} \delta_1 & 0 \\ 0 & \delta_2 \end{pmatrix}, \quad U = e^{i\alpha} \begin{pmatrix} e^{i\beta} \cos(\theta) & e^{i\gamma} \sin(\theta) \\ -e^{-i\gamma} \sin(\theta) & e^{-i\beta} \cos(\theta) \end{pmatrix}, \quad (\text{A.2})$$

where $\delta_1, \delta_2 \in \mathbb{C} \setminus \{0\}$ and $\alpha, \beta, \gamma, \theta \in \mathbb{R}$, such that

$$DAU = \begin{pmatrix} \delta_1(a_1e^{i(\alpha+\beta)} \cos(\theta) - a_2e^{i(\alpha-\gamma)} \sin(\theta)) & \delta_1(a_1e^{i(\alpha+\gamma)} \sin(\theta) + a_2e^{i(\alpha-\beta)} \cos(\theta)) \\ \delta_2(a_3e^{i(\alpha+\beta)} \cos(\theta) - a_4e^{i(\alpha-\gamma)} \sin(\theta)) & \delta_2(a_3e^{i(\alpha+\gamma)} \sin(\theta) + a_4e^{i(\alpha-\beta)} \cos(\theta)) \end{pmatrix}, \quad (\text{A.3})$$

$$UAD' = \begin{pmatrix} \delta'_1 (a_1e^{i(\alpha+\beta)} \cos(\theta) + a_3e^{i(\alpha+\gamma)} \sin(\theta)) & \delta'_2 (a_2e^{i(\alpha+\beta)} \cos(\theta) + a_4e^{i(\alpha+\gamma)} \sin(\theta)) \\ \delta'_1 (a_3e^{i(\alpha-\beta)} \cos(\theta) - a_1e^{i(\alpha-\gamma)} \sin(\theta)) & \delta'_2 (a_4e^{i(\alpha-\beta)} \cos(\theta) - a_2e^{i(\alpha-\gamma)} \sin(\theta)) \end{pmatrix}, \quad (\text{A.4})$$

$$DAD' = \begin{pmatrix} \delta_1 \delta'_1 a_1 & \delta_1 \delta'_2 a_2 \\ \delta_2 \delta'_1 a_3 & \delta_2 \delta'_2 a_4 \end{pmatrix}. \quad (\text{A.5})$$

Eigenvalues: The eigenvalues of A are found from

$$\det(A - \lambda I) = (a_1 - \lambda)(a_4 - \lambda) - a_2 a_3 = 0, \quad (\text{A.6})$$

yielding

$$\lambda_{\pm} = \frac{a_1 + a_4 \pm \sqrt{(a_1 - a_4)^2 + 4a_2 a_3}}{2}. \quad (\text{A.7})$$

Singular Values: The singular values of A are the square roots of the eigenvalues of

$$A^\dagger A = \begin{pmatrix} |a_1|^2 + |a_3|^2 & \overline{a_1} a_2 + \overline{a_3} a_4 \\ a_1 \overline{a_2} + a_3 \overline{a_4} & |a_2|^2 + |a_4|^2 \end{pmatrix}. \quad (\text{A.8})$$

Since

$$\text{tr}(A^\dagger A) = |a_1|^2 + |a_2|^2 + |a_3|^2 + |a_4|^2, \quad \det(A^\dagger A) = |a_1 a_4 - a_2 a_3|^2, \quad (\text{A.9})$$

the eigenvalues of $A^\dagger A$ are obtained using Eq. (A.7) as λ'_{\pm} , which gives us the singular values of A as $\sigma_{\pm} = \sqrt{\lambda'_{\pm}}$

$$\sigma_{\pm} = \sqrt{\frac{|a_1|^2 + |a_2|^2 + |a_3|^2 + |a_4|^2 \pm \sqrt{(|a_1|^2 + |a_2|^2 + |a_3|^2 + |a_4|^2)^2 - 4|a_1 a_4 - a_2 a_3|^2}}{2}}. \quad (\text{A.10})$$

LUI-singular values: The left diagonal scale function matrix in Eq. (2.3) is defined using the Euclidean norm for each row

$$D^L(A) = \text{diag} \left(\frac{1}{\sqrt{|a_1|^2 + |a_2|^2}}, \frac{1}{\sqrt{|a_3|^2 + |a_4|^2}} \right). \quad (\text{A.11})$$

The balanced matrix A^L is given by

$$A^L = D^L \cdot A = \begin{bmatrix} \frac{a_1}{\sqrt{|a_1|^2 + |a_2|^2}} & \frac{a_2}{\sqrt{|a_1|^2 + |a_2|^2}} \\ \frac{a_3}{\sqrt{|a_3|^2 + |a_4|^2}} & \frac{a_4}{\sqrt{|a_3|^2 + |a_4|^2}} \end{bmatrix}. \quad (\text{A.12})$$

The singular values of the balanced matrix A^L , which are the left unit-invariant singular values σ_{\pm}^L of A , are (using Eq. (A.10))

$$\sigma_{\pm}^L = \sqrt{1 \pm \sqrt{1 - \frac{|a_1 a_4 - a_2 a_3|^2}{(|a_1|^2 + |a_2|^2)(|a_3|^2 + |a_4|^2)}}}. \quad (\text{A.13})$$

We can verify that these values are invariant under transformation (A.3). In fact, we can prove more generally that for any matrix $A \in \mathbb{C}^{m \times n}$ with any nonsingular diagonal $D \in \mathbb{C}^{m \times m}$ and any unitary $U \in \mathbb{C}^{n \times n}$

$$\sigma^L(A) = \sigma^L(DAU). \quad (\text{A.14})$$

Proof: Let $B := DAU$. Row i of B equals

$$B(i, :) = d_i A(i, :) U. \quad (\text{A.15})$$

Now take Euclidean norms and use the facts that $\|cx\|_2 = |c|\|x\|_2$ and that $\|xU\|_2 = \|x\|_2$ for unitary U ,

$$\|B(i, :)\|_2 = \|d_i A(i, :) U\|_2 = |d_i| \|A(i, :) U\|_2 = |d_i| \|A(i, :)\|_2 = |d_i| r_i. \quad (\text{A.16})$$

So if $r_i > 0$, then $(D^L(B))_{ii} = 1/(|d_i|r_i)$. Using the diagonal expression above,

$$B^L = D^L(B) B = \text{diag}\left(\frac{1}{|d_i|r_i}\right) \text{diag}(d_i) A U. \quad (\text{A.17})$$

Factor the product of the two diagonal matrices

$$\text{diag}\left(\frac{1}{|d_i|r_i}\right) \text{diag}(d_i) = \underbrace{\text{diag}\left(\frac{d_i}{|d_i|}\right)}_{:=\Phi \text{ diagonal unitary}} \underbrace{\text{diag}\left(\frac{1}{r_i}\right)}_{=D^L(A)}, \quad (\text{A.18})$$

and the $r_i = 0$ case is handled analogously with $(D^L(B))_{ii} = 1 = (D^L(A))_{ii}$ from definition. Therefore

$$B^L = \Phi D^L(A) A U = \Phi A^L U. \quad (\text{A.19})$$

Φ is unitary (diagonal with entries of modulus 1), and U is unitary, hence using property of usual singular values

$$\sigma(B^L) = \sigma(\Phi A^L U) = \sigma(A^L). \quad (\text{A.20})$$

By definition $\sigma^L(A) = \sigma(A^L)$ and $\sigma^L(B) = \sigma(B^L)$. Thus $\sigma^L(DAU) = \sigma^L(A)$. An entirely analogous argument holds for RUISVD using columns instead of rows.

RUI-singular values: The right diagonal scale function matrix Eq. (2.8) is defined using the Euclidean norm for each column

$$D^R(A) = \text{diag}\left(\frac{1}{\sqrt{|a_1|^2 + |a_3|^2}}, \frac{1}{\sqrt{|a_2|^2 + |a_4|^2}}\right). \quad (\text{A.21})$$

The balanced matrix A^R is given by

$$A^R = A \cdot D^R = \begin{bmatrix} \frac{a_1}{\sqrt{|a_1|^2 + |a_3|^2}} & \frac{a_2}{\sqrt{|a_2|^2 + |a_4|^2}} \\ \frac{a_3}{\sqrt{|a_1|^2 + |a_3|^2}} & \frac{a_4}{\sqrt{|a_2|^2 + |a_4|^2}} \end{bmatrix}. \quad (\text{A.22})$$

The singular values of the balanced matrix A^R , which are the right unit-invariant singular values σ_{\pm}^R of A , are (using Eq. (A.10))

$$\sigma_{\pm}^R = \sqrt{1 \pm \sqrt{1 - \frac{|a_1a_4 - a_2a_3|^2}{(|a_1|^2 + |a_3|^2)(|a_2|^2 + |a_4|^2)}}}. \quad (\text{A.23})$$

We can verify that these values are invariant under transformation (A.4).

BUI-singular values: Define

$$K = \log(\text{Abs}[A]) = \begin{bmatrix} \ln|a_1| & \ln|a_2| \\ \ln|a_3| & \ln|a_4| \end{bmatrix}, \quad J_2 = \frac{1}{2} \begin{bmatrix} 1 & 1 \\ 1 & 1 \end{bmatrix}, \quad (\text{A.24})$$

where $J_p = \begin{bmatrix} \frac{1}{p} \\ p \end{bmatrix}_{p \times p}$. So for $m \times n$ matrix we compute

$$Q = J_m K J_n - K J_n - J_m K. \quad (\text{A.25})$$

Here, dimensions $m = n = 2$, and we set

$$P[A] = \exp(Q) = \begin{bmatrix} |a_1^{-\frac{3}{4}} a_2^{-\frac{1}{4}} a_3^{-\frac{1}{4}} a_4^{\frac{1}{4}}| & |a_1^{-\frac{1}{4}} a_2^{-\frac{3}{4}} a_3^{\frac{1}{4}} a_4^{-\frac{1}{4}}| \\ |a_1^{-\frac{1}{4}} a_2^{\frac{1}{4}} a_3^{-\frac{3}{4}} a_4^{-\frac{1}{4}}| & |a_1^{\frac{1}{4}} a_2^{-\frac{1}{4}} a_3^{-\frac{1}{4}} a_4^{-\frac{3}{4}}| \end{bmatrix}. \quad (\text{A.26})$$

Writing $P[A]$ in the form $\mathbf{x}\mathbf{y}^\top$ we pick the top-left entry (index (1, 1)) as the reference scale. Namely,

$$x_1 = 1, \quad x_2 = \frac{P[A]_{2,1}}{P[A]_{1,1}}, \quad y_1 = P[A]_{1,1}, \quad y_2 = P[A]_{1,2}. \quad (\text{A.27})$$

Then

$$D^{\text{BL}} = \text{diag}(x_1, x_2), \quad D^{\text{BR}} = \text{diag}(y_1, y_2). \quad (\text{A.28})$$

A direct exponent check yields

$$D^{\text{BL}} = \begin{bmatrix} 1 & 0 \\ 0 & \sqrt{\frac{|a_1 a_2|}{|a_3 a_4|}} \end{bmatrix}, \quad D^{\text{BR}} = \begin{bmatrix} |a_1^{-\frac{3}{4}} a_2^{-\frac{1}{4}} a_3^{-\frac{1}{4}} a_4^{\frac{1}{4}}| & 0 \\ 0 & |a_1^{-\frac{1}{4}} a_2^{-\frac{3}{4}} a_3^{\frac{1}{4}} a_4^{-\frac{1}{4}}| \end{bmatrix}. \quad (\text{A.29})$$

The balanced matrix $A^{\text{B}} = D^{\text{BL}} A D^{\text{BR}}$ is

$$A^{\text{B}} = \begin{pmatrix} a_1 |a_1|^{-3/4} |a_4/(a_2 a_3)|^{1/4} & a_2 |a_2|^{-3/4} |a_3/(a_1 a_4)|^{1/4} \\ a_3 |a_3|^{-3/4} |a_2/(a_1 a_4)|^{1/4} & a_4 |a_4|^{-3/4} |a_1/(a_2 a_3)|^{1/4} \end{pmatrix} \quad (\text{A.30})$$

The BUI-singular values of A are the singular values of A^{B} (using Eq. (A.10))

$$\sigma_{\pm}^{\text{B}} = \sqrt{\left(\sqrt{\frac{|a_1 a_4|}{|a_2 a_3|}} + \sqrt{\frac{|a_2 a_3|}{|a_1 a_4|}} \right) \pm \sqrt{\left(\sqrt{\frac{|a_1 a_4|}{|a_2 a_3|}} + \sqrt{\frac{|a_2 a_3|}{|a_1 a_4|}} \right)^2 - \frac{|a_1 a_4 - a_2 a_3|^2}{|a_1 a_2 a_3 a_4|}}}, \quad (\text{A.31})$$

which further simplifies to

$$\sigma_{\pm}^{\text{B}} = \sqrt[4]{\frac{|a_1 a_4|}{|a_2 a_3|}} \pm \sqrt[4]{\frac{|a_2 a_3|}{|a_1 a_4|}}, \quad \text{when } a_i \in \mathbb{R}_+. \quad (\text{A.32})$$

We can verify that these values are invariant under transformation (A.5). More generally, for any given matrix $A \in \mathbb{C}^{m \times n}$, the routine below computes positive diagonal scalings $D^{\text{BL}} = \text{diag}(d_\ell)$ and $D^{\text{BR}} = \text{diag}(d_r)$ such that

$$A^{\text{B}} = D^{\text{BL}} A D^{\text{BR}} \quad (\text{A.33})$$

has (on the support pattern of A) approximately unit geometric mean per row and per column in magnitude. The *UI singular values* of A are then defined as the singular values of this balanced matrix A^B . This is the implementation used to generate the BUISVD curves in our numerical plots. It is a Python adaptation of the MATLAB code provided in [27, Appendix C].

Python code for BUISVD

```

import numpy as np

def dscale(A, tol=1e-15, max_iters=None, return_iters=False):
    A = np.asarray(A)
    if A.ndim != 2:
        raise ValueError("A must be a 2D array.")

    m, n = A.shape
    it = 0

    if np.iscomplexobj(A):
        A = A.astype(np.complex128, copy=False)
        A_abs = np.abs(A)
        A_phase = np.zeros((m, n), dtype=np.complex128)
        np.divide(A, A_abs, out=A_phase, where=(A_abs != 0))
    else:
        A = A.astype(np.float64, copy=False)
        A_abs = np.abs(A)
        A_phase = np.sign(A)
        A_phase[A == 0] = 0.0

    L = np.zeros((m, n), dtype=np.float64)
    M = np.ones((m, n), dtype=np.float64)

    nz = (A_abs > 0.0)
    L[nz] = np.log(A_abs[nz])
    M[~nz] = 0.0

    r = np.sum(M, axis=1)
    c = np.sum(M, axis=0)

    u = np.zeros((m, 1), dtype=np.float64)
    v = np.zeros((1, n), dtype=np.float64)

    dx = 2.0 * tol
    while dx > tol and (max_iters is None or it < max_iters):
        it += 1

        idx = (c > 0)

```

```

p = np.sum(L[:, idx], axis=0) / c[idx]
L[:, idx] = L[:, idx] - (p[None, :] * M[:, idx])
v[:, idx] = v[:, idx] - p
dx = np.mean(np.abs(p))

idx = (r > 0)
p = np.sum(L[idx, :], axis=1) / r[idx]
L[idx, :] = L[idx, :] - (p[:, None] * M[idx, :])
u[idx, 0] = u[idx, 0] - p
dx = dx + np.mean(np.abs(p))

d_l = np.exp(u)
d_r = np.exp(v)
A_U = A_phase * np.exp(L)

if return_iters:
    return A_U, d_l, d_r, it
return A_U, d_l, d_r

def bui_singular_values(A, tol=1e-15, max_iters=None):
    A_U, _, _ = dscale(A, tol=tol, max_iters=max_iters)
    return np.linalg.svd(A_U, compute_uv=False)

def usvd(A, tol=1e-15, max_iters=None):
    return bui_singular_values(A, tol=tol, max_iters=max_iters)

```

B Results from Random Matrix Theory

Here we collect known results from Random Matrix Theory and further prove certain Lemmas, which are required for proving Theorems 2.1 to 2.4.

Notation and conventions. For an $n \times n$ Hermitian matrix M with eigenvalues $\lambda_1(M), \dots, \lambda_n(M) \in \mathbb{R}$, its *empirical spectral distribution (ESD)* is

$$\text{ESD}(M) := \frac{1}{n} \sum_{i=1}^n \delta_{\lambda_i(M)}. \quad (\text{B.1})$$

We write $\mu_n \Rightarrow \mu$ for weak convergence of probability measures on \mathbb{R} . For a probability measure μ on \mathbb{R} , its *Stieltjes transform* is

$$m_\mu(z) := \int_{\mathbb{R}} \frac{1}{x-z} d\mu(x), \quad z \in \mathbb{C}^+ := \{z \in \mathbb{C} : \Im z > 0\}. \quad (\text{B.2})$$

For a Hermitian M , we write $m_M(z) := \frac{1}{n} \text{Tr}(M - zI)^{-1}$; then m_M is the Stieltjes transform of $\text{ESD}(M)$. We use the Orlicz norms

$$\|X\|_{\psi_1} := \inf\{t > 0 : \mathbb{E} e^{|X|/t} \leq 2\}, \quad \|X\|_{\psi_2} := \inf\{t > 0 : \mathbb{E} e^{|X|^2/t^2} \leq 2\}. \quad (\text{B.3})$$

A (real) random variable is *sub-Gaussian* if $\|X\|_{\psi_2} < \infty$ and *subexponential* if $\|X\|_{\psi_1} < \infty$. For complex X , we interpret sub-Gaussian/subexponential in the same way with $|X|$ (equivalently, it suffices that $\Re X$ and $\Im X$ are sub-Gaussian). Throughout, for complex entries we use the convention $\mathbb{E}|X_{ij}|^2 = 1$ when we say “variance 1”. We write A^\dagger for the conjugate transpose of a complex matrix A , and $\|A\|_{\mathcal{O}}$ for its operator (spectral) norm. We write $\mathbb{P}(\cdot)$ for probability. For $\beta \in \{1, 2\}$ we use the shorthand g_β for a standard real/complex Gaussian: $g_1 \sim \mathcal{N}(0, 1)$ and $g_2 \sim \mathcal{CN}(0, 1)$ (circular, with $\mathbb{E}|g_2|^2 = 1$).

Theorem B.1 ([30, Cor. 2.8.4]). *If X_1, \dots, X_n are independent, mean-zero, subexponential random variables with $c_0 := \max_i \|X_i\|_{\psi_1}$, then for all $t \geq 0$,*

$$\mathbb{P}\left(\frac{1}{n} \left| \sum_{i=1}^n X_i \right| \geq t\right) \leq 2 \exp\left[-nc \min\left(\frac{t^2}{c_0^2}, \frac{t}{c_0}\right)\right]. \quad (\text{B.4})$$

Theorem B.2 (Marchenko-Pastur law [64, Thms. 3.6 & 3.7]). *If X_n is $p \times n$ with i.i.d. entries of mean 0, variance σ^2 , and $p/n \rightarrow y \in (0, \infty)$, then the empirical spectral distribution of $\frac{1}{n} X_n X_n^\dagger$ converges almost surely to $MP(y, \sigma^2)$.*

Theorem B.3 ([64, Thms. 5.10 & 5.11]). *Under the assumptions of Theorem B.2 and finite fourth moment,*

$$\lambda_{\max}\left(\frac{1}{n} X_n X_n^\dagger\right) \xrightarrow{\text{a.s.}} \sigma^2(1 + \sqrt{y})^2, \quad \lambda_{\min} \xrightarrow{\text{a.s.}} \sigma^2(1 - \sqrt{y})^2 \quad (y \leq 1). \quad (\text{B.5})$$

Theorem B.4 (Wigner semicircle [65, Thms. 2.4.2 & 2.3.24]). *Let H_n be GOE/GUE with the $1/\sqrt{n}$ scaling. Then the eigenvalue ESD of H_n converges almost surely to the semicircle law on $[-2, 2]$, and $\|H_n\|_{\mathcal{O}} \rightarrow 2$ almost surely.*

B.1 Derived Lemmas

Lemma B.5. *Let T_n be random $n \times n$ matrices and $H_n := T_n T_n^\dagger$. If $\text{ESD}(H_n) \Rightarrow F$ almost surely with $\text{supp}(F) \subset [0, b]$, then the empirical measure of singular values of T_n converges almost surely to the pushforward $F \circ f^{-1}$ under $f(x) = \sqrt{x}$, supported on $[0, \sqrt{b}]$.*

Proof. Let $\lambda_1(H_n), \dots, \lambda_n(H_n)$ be the eigenvalues of $H_n := T_n T_n^\dagger$. The singular values of T_n are $\sigma_i(T_n) = \sqrt{\lambda_i(H_n)}$. Let $\mu_n := \text{ESD}(H_n)$ and let ν_n be the empirical measure of the singular values of T_n . Then for every bounded continuous function $g : [0, \infty) \rightarrow \mathbb{R}$,

$$\int g(s) d\nu_n(s) = \frac{1}{n} \sum_{i=1}^n g(\sigma_i(T_n)) = \frac{1}{n} \sum_{i=1}^n g(\sqrt{\lambda_i(H_n)}) = \int g(\sqrt{x}) d\mu_n(x). \quad (\text{B.6})$$

If $\mu_n \Rightarrow F$ almost surely and $x \mapsto g(\sqrt{x})$ is bounded and continuous on $[0, \infty)$, then $\int g(\sqrt{x}) d\mu_n(x) \rightarrow \int g(\sqrt{x}) dF(x)$ almost surely. Hence $\nu_n \Rightarrow F \circ f^{-1}$ almost surely where $f(x) = \sqrt{x}$, and $\text{supp}(F) \subset [0, b]$ implies $\text{supp}(F \circ f^{-1}) \subset [0, \sqrt{b}]$. \square

Lemma B.6. *Let $A_n = (1/\sqrt{n}) X_n$ where the entries $\{X_{ij}\}$ of X_n are i.i.d., mean 0, variance 1, and sub-Gaussian. Define the row and column Euclidean (ℓ^2) norms*

$$r_i := \|A_n(i, :)\|_2, \quad c_j := \|A_n(:, j)\|_2. \quad (\text{B.7})$$

There exists a constant $C > 0$ (independent of n) such that, for all sufficiently large n ,

$$\mathbb{P}\left(\max_{1 \leq i \leq n} |r_i - 1| > C\sqrt{\frac{\log n}{n}}\right) \leq n^{-10}, \quad \mathbb{P}\left(\max_{1 \leq j \leq n} |c_j - 1| > C\sqrt{\frac{\log n}{n}}\right) \leq n^{-10}. \quad (\text{B.8})$$

Proof. Fix i . Since $A_n = (1/\sqrt{n})X_n$, with $\mathbb{E}(X_{ij}) = 0$ and $\mathbb{E}|X_{ij}|^2 - |\mathbb{E}X_{ij}|^2 = \text{Var}(X_{ij}) = 1$, we get

$$r_i^2 = \|A_n(i, :)\|_2^2 = \frac{1}{n} \sum_{k=1}^n |X_{ik}|^2 \quad \text{and} \quad \mathbb{E}[r_i^2] = \frac{1}{n} \sum_{k=1}^n \mathbb{E}|X_{ik}|^2 = 1. \quad (\text{B.9})$$

Define centered variables $Z_{ik} := |X_{ik}|^2 - 1$ so that

$$r_i^2 - 1 = \frac{1}{n} \sum_{k=1}^n Z_{ik}. \quad (\text{B.10})$$

Because X_{ik} is sub-Gaussian, Z_{ik} is *subexponential* [30, Lem. 2.7.4]. Let $c_0 := \|Z_{i1}\|_{\psi_1}$; since the Z_{ik} are i.i.d. in k , we have $\max_{1 \leq k \leq n} \|Z_{ik}\|_{\psi_1} \leq c_0$. So Theorem B.1 yields

$$\mathbb{P}(|r_i^2 - 1| > u) = \mathbb{P}\left(\left|\frac{1}{n} \sum_{k=1}^n Z_{ik}\right| > u\right) \leq 2 \exp\left[-c n \min\left(\frac{u^2}{c_0^2}, \frac{u}{c_0}\right)\right]. \quad (\text{B.11})$$

We now choose the deviation level

$$u := c_1 \sqrt{\frac{\log n}{n}}, \quad (\text{B.12})$$

with a constant $c_1 > 0$ to be specified. For n large enough, $u/c_0 \leq 1$, so

$$\min\left(\frac{u^2}{c_0^2}, \frac{u}{c_0}\right) = \frac{u^2}{c_0^2}. \quad (\text{B.13})$$

Substitute this u into Eq. (B.11):

$$\mathbb{P}\left(|r_i^2 - 1| > c_1 \sqrt{\frac{\log n}{n}}\right) \leq 2 \exp\left[-c n \cdot \frac{u^2}{c_0^2}\right] = 2 \exp\left[-\frac{cc_1^2}{c_0^2} \log n\right]. \quad (\text{B.14})$$

Because constants are free to pick in a tail bound, we choose c_1 large enough such that⁸

$$\frac{cc_1^2}{c_0^2} \geq 12 \implies \mathbb{P}\left(|r_i^2 - 1| > c_1 \sqrt{\frac{\log n}{n}}\right) \leq 2 \exp(-12 \log n) = 2n^{-12}. \quad (\text{B.15})$$

Define events $E_i := \{|r_i^2 - 1| > c_1 \sqrt{\frac{\log n}{n}}\}$. Then

$$\left\{ \max_{1 \leq i \leq n} |r_i^2 - 1| > c_1 \sqrt{\frac{\log n}{n}} \right\} = \bigcup_{i=1}^n E_i. \quad (\text{B.16})$$

⁸For notational convenience we choose 12, can be any large value.

By the union bound $\mathbb{P}(\cup_{i=1}^n E_i) \leq \sum_{i=1}^n \mathbb{P}(E_i)$ and the previous estimate,

$$\mathbb{P}\left(\max_{1 \leq i \leq n} |r_i^2 - 1| > c_1 \sqrt{\frac{\log n}{n}}\right) \leq \sum_{i=1}^n 2n^{-12} = 2n \cdot n^{-12} = 2n^{-11} \leq n^{-10} \quad (\text{B.17})$$

for all sufficiently large n . Now,

$$|r_i - 1| = \frac{|r_i^2 - 1|}{\sqrt{r_i^2 + 1}} = \frac{|r_i^2 - 1|}{r_i + 1}. \quad (\text{B.18})$$

Therefore, always (since $r_i \geq 0$),

$$|r_i - 1| \leq |r_i^2 - 1|. \quad (\text{B.19})$$

So we have the implication

$$\left\{ \max_{1 \leq i \leq n} |r_i - 1| > c_1 \sqrt{\frac{\log n}{n}} \right\} \subseteq \left\{ \max_{1 \leq i \leq n} |r_i^2 - 1| > c_1 \sqrt{\frac{\log n}{n}} \right\}. \quad (\text{B.20})$$

Therefore, using Eq. (B.17)

$$\mathbb{P}\left(\max_{1 \leq i \leq n} |r_i - 1| > C \sqrt{\frac{\log n}{n}}\right) \leq n^{-10}. \quad (\text{B.21})$$

An entirely analogous argument, with rows replaced by columns, yields the bound for c_j . \square

Corollary B.7. *For all sufficiently large n , with probability at least $1 - Cn^{-10}$ there exist diagonal Δ_n^L, Δ_n^R such that*

$$D_n^L = I + \Delta_n^L, \quad D_n^R = I + \Delta_n^R, \quad \|\Delta_n^L\|_{\mathcal{O}}, \|\Delta_n^R\|_{\mathcal{O}} \leq C \sqrt{\frac{\log n}{n}}. \quad (\text{B.22})$$

Proof. By Lemma B.6, with probability at least $1 - Cn^{-10}$ we have

$$\max_i |r_i - 1| \leq C_0 \sqrt{\frac{\log n}{n}}, \quad \max_j |c_j - 1| \leq C_0 \sqrt{\frac{\log n}{n}}. \quad (\text{B.23})$$

On this event, for every n such that $C_0 \sqrt{\frac{\log n}{n}} \leq \frac{1}{2}$, we have $\min_i r_i \geq \frac{1}{2}$ and $\min_j c_j \geq \frac{1}{2}$. Hence

$$|(D_n^L)_{ii} - 1| = \left| \frac{1}{r_i} - 1 \right| = \frac{|1 - r_i|}{r_i} \leq 2|r_i - 1|, \quad |(D_n^R)_{jj} - 1| \leq 2|c_j - 1|. \quad (\text{B.24})$$

Define $\Delta_n^L := D_n^L - I$ and $\Delta_n^R := D_n^R - I$. Since these are diagonal,

$$\|\Delta_n^L\|_{\mathcal{O}} = \max_i |(D_n^L)_{ii} - 1| \leq C \sqrt{\frac{\log n}{n}}, \quad \|\Delta_n^R\|_{\mathcal{O}} \leq C \sqrt{\frac{\log n}{n}}. \quad (\text{B.25})$$

\square

Lemma B.8. *If $D = I + \Delta$ is diagonal and $D = D^\dagger$ (e.g. real diagonal), then for any A ,*

$$\|DAA^\dagger D^\dagger - AA^\dagger\|_{\mathcal{O}} \leq (2\|\Delta\|_{\mathcal{O}} + \|\Delta\|_{\mathcal{O}}^2) \|A\|_{\mathcal{O}}^2. \quad (\text{B.26})$$

Proof. Let $M := AA^\dagger$. Then

$$DMD - M = (I + \Delta)M(I + \Delta) - M = \Delta M + M\Delta + \Delta M\Delta. \quad (\text{B.27})$$

Hence, by the triangle inequality and submultiplicativity of $\|\cdot\|_{\mathcal{O}}$,

$$\|DMD - M\|_{\mathcal{O}} \leq \|\Delta M\|_{\mathcal{O}} + \|M\Delta\|_{\mathcal{O}} + \|\Delta M\Delta\|_{\mathcal{O}} \quad (\text{B.28})$$

$$\leq \|\Delta\|_{\mathcal{O}}\|M\|_{\mathcal{O}} + \|M\|_{\mathcal{O}}\|\Delta\|_{\mathcal{O}} + \|\Delta\|_{\mathcal{O}}\|M\|_{\mathcal{O}}\|\Delta\|_{\mathcal{O}} \quad (\text{B.29})$$

$$= (2\|\Delta\|_{\mathcal{O}} + \|\Delta\|_{\mathcal{O}}^2) \|M\|_{\mathcal{O}}. \quad (\text{B.30})$$

Finally, $\|M\|_{\mathcal{O}} = \|AA^\dagger\|_{\mathcal{O}} \leq \|A\|_{\mathcal{O}}\|A^\dagger\|_{\mathcal{O}} = \|A\|_{\mathcal{O}}^2$, which proves the claim. \square

Lemma B.9. *Let $M, N \in \mathbb{C}^{n \times n}$ be Hermitian and set $E := N - M$. For $z = x + iy$ with $y > 0$, define the resolvents $R_M(z) := (M - zI)^{-1}$, $R_N(z) := (N - zI)^{-1}$ and their normalised traces $m_M(z) := \frac{1}{n} \text{Tr}R_M(z)$, $m_N(z) := \frac{1}{n} \text{Tr}R_N(z)$. Then*

$$|m_N(z) - m_M(z)| \leq \frac{\|E\|_{\mathcal{O}}}{y^2}. \quad (\text{B.31})$$

Consequently, if $\|E_n\|_{\mathcal{O}} \rightarrow 0$ and $m_{M_n}(z) \rightarrow m(z)$ for every fixed $z \in \mathbb{C}^+$, then $m_{N_n}(z) \rightarrow m(z)$ for every fixed $z \in \mathbb{C}^+$ as well. In particular, M_n and N_n have the same limiting ESD (by uniqueness of Stieltjes transforms).

Proof. We use the resolvent identity. For $E := N - M$,

$$\begin{aligned} R_N(z) - R_M(z) &= (N - zI)^{-1} - (M - zI)^{-1} \\ &= (M - zI)^{-1}((M - zI) - (N - zI))(N - zI)^{-1} \\ &= -R_M(z)E R_N(z). \end{aligned} \quad (\text{B.32})$$

Therefore

$$|m_N(z) - m_M(z)| = \left| \frac{1}{n} \text{Tr}(R_N(z) - R_M(z)) \right| \leq \frac{1}{n} |\text{Tr}(R_M(z)ER_N(z))|. \quad (\text{B.33})$$

Using the bound $|\text{Tr}(X)| \leq n\|X\|_{\mathcal{O}}$ and submultiplicativity of the operator norm,

$$|\text{Tr}(R_M(z)ER_N(z))| \leq n\|R_M(z)ER_N(z)\|_{\mathcal{O}} \leq n\|R_M(z)\|_{\mathcal{O}}\|E\|_{\mathcal{O}}\|R_N(z)\|_{\mathcal{O}}. \quad (\text{B.34})$$

Therefore

$$|m_N(z) - m_M(z)| \leq \|R_M(z)\|_{\mathcal{O}}\|E\|_{\mathcal{O}}\|R_N(z)\|_{\mathcal{O}}. \quad (\text{B.35})$$

Diagonalise $M = U\Lambda U^\dagger$ with $\Lambda = \text{diag}(\lambda_1, \dots, \lambda_n) \in \mathbb{R}^{n \times n}$. Then

$$R_M(z) = (M - zI)^{-1} = U(\Lambda - zI)^{-1}U^\dagger, \quad \|R_M(z)\|_{\mathcal{O}} = \max_{1 \leq k \leq n} \frac{1}{|\lambda_k - z|}. \quad (\text{B.36})$$

Because $z = x + iy$ with $y > 0$ and $\lambda_k \in \mathbb{R}$, $|\lambda_k - z| \geq \Im z = y$, hence $\|R_M(z)\|_{\mathcal{O}} \leq 1/y$. The same holds for $R_N(z)$. Therefore

$$|m_N(z) - m_M(z)| \leq \frac{1}{y} \|E\|_{\mathcal{O}} \frac{1}{y} = \frac{\|E\|_{\mathcal{O}}}{y^2}. \quad (\text{B.37})$$

Finally, if $\|E_n\|_{\mathcal{O}} \rightarrow 0$ and $m_{M_n}(z) \rightarrow m(z)$ for every fixed $z \in \mathbb{C}^+$, then the bound Eq. (B.31) yields $m_{N_n}(z) \rightarrow m(z)$ for every fixed $z \in \mathbb{C}^+$ as well. By uniqueness of Stieltjes transforms, M_n and N_n have the same limiting ESD. \square

Proposition B.10. *For any square matrix $A = (a_{ij})$ with non-zero entries, we obtain A^B and set*

$$m_i := \frac{1}{n} \sum_{k=1}^n \log |a_{ik}|, \quad n_j := \frac{1}{n} \sum_{k=1}^n \log |a_{kj}|, \quad \bar{m} := \frac{1}{n^2} \sum_{i,j=1}^n \log |a_{ij}|. \quad (\text{B.38})$$

Then the unknowns $(\log d_i)_{i=1}^n$ and $(\log r_j)_{j=1}^n$ with $d_i, r_j \in \mathbb{R}_{>0}$ (equivalently $\log d_i, \log r_j \in \mathbb{R}$) that satisfy Eq. (2.14) are precisely

$$\log d_i = -m_i - \alpha, \quad \log r_j = -n_j - \beta, \quad \alpha + \beta = -\bar{m} \quad (\text{B.39})$$

for some real constants α, β . The pair (α, β) is a one-parameter scale family. The symmetric scale is $\alpha = \beta = -\bar{m}/2$, equivalently

$$\frac{1}{n} \sum_{i=1}^n \log d_i = \frac{1}{n} \sum_{j=1}^n \log r_j. \quad (\text{B.40})$$

Proof. Write $A_{ij}^B = d_i A_{ij} r_j$ (entrywise). Then

$$\log |A_{ij}^B| = \log d_i + \log |A_{ij}| + \log r_j. \quad (\text{B.41})$$

Fix i and average over j :

$$\frac{1}{n} \sum_{j=1}^n \log |A_{ij}^B| = \log d_i + \frac{1}{n} \sum_{j=1}^n \log |A_{ij}| + \frac{1}{n} \sum_{j=1}^n \log r_j = \log d_i + m_i + \alpha, \quad (\text{B.42})$$

where we set $\alpha := \frac{1}{n} \sum_{j=1}^n \log r_j$. The row constraint Eq. (2.14) gives

$$\log d_i = -m_i - \alpha \quad (1 \leq i \leq n). \quad (\text{B.43})$$

Fix j and average over i :

$$\frac{1}{n} \sum_{i=1}^n \log |A_{ij}^B| = \frac{1}{n} \sum_{i=1}^n \log d_i + \frac{1}{n} \sum_{i=1}^n \log |A_{ij}| + \log r_j = \beta + n_j + \log r_j, \quad (\text{B.44})$$

where $\beta := \frac{1}{n} \sum_{i=1}^n \log d_i$. The column constraint gives

$$\log r_j = -n_j - \beta \quad (1 \leq j \leq n). \quad (\text{B.45})$$

Average Eq. (B.43) over i or Eq. (B.45) over j to get the single constraint

$$\alpha + \beta = -\bar{m}. \quad (\text{B.46})$$

This is exactly the displayed solution family. The *symmetric scale* chooses $\alpha = \beta = -\bar{m}/2$, which forces

$$\frac{1}{n} \sum_i \log d_i = \beta = -\bar{m}/2 = \alpha = \frac{1}{n} \sum_j \log r_j. \quad (\text{B.47})$$

□

Remark B.1. For continuous entry laws (e.g. Gaussian Ginibre/Wigner), $\mathbb{P}(a_{ij} = 0) = 0$, so the logarithms are well-defined almost surely and our BUISVD scalings are a.s. well-posed. One can always regularise by replacing $|a_{ij}|$ with $\max\{|a_{ij}|, \varepsilon\}$ and then send $\varepsilon \downarrow 0$ if desired.

Lemma B.11. Let $a_{ij} = X_{ij}/\sqrt{n}$ where X_{ij} are i.i.d. real or complex random variables with mean 0, variance 1, sub-Gaussian tails, $\mathbb{P}(X_{ij} = 0) = 0$, and a small-ball bound near 0, namely: there exist $\alpha > 0$ and $C_0 < \infty$ such that $\mathbb{P}(|X_{ij}| \leq t) \leq C_0 t^\alpha$ for all $t \in (0, 1)$. Define the row/column/grand log averages (as in Eq. (B.38))

$$m_i := \frac{1}{n} \sum_{k=1}^n \log |a_{ik}|, \quad n_j := \frac{1}{n} \sum_{k=1}^n \log |a_{kj}|, \quad \bar{m} := \frac{1}{n^2} \sum_{i,j=1}^n \log |a_{ij}|. \quad (\text{B.48})$$

Set $c_\star := \mathbb{E} \log |X_{11}|$ (finite under the assumptions above). Then there exists $C > 0$ such that, for all sufficiently large n , with probability at least $1 - Cn^{-10}$,

$$\max_i \left| m_i - (c_\star - \frac{1}{2} \log n) \right|, \quad \max_j \left| n_j - (c_\star - \frac{1}{2} \log n) \right|, \quad \left| \bar{m} - (c_\star - \frac{1}{2} \log n) \right| \leq C \sqrt{\frac{\log n}{n}}. \quad (\text{B.49})$$

Proof. We do rows; columns are identical; \bar{m} is a single average over n^2 terms. First, under the stated assumptions $c_\star = \mathbb{E} \log |X_{11}|$ is finite. Also, by increasing C_0 if necessary, we may assume the small-ball bound $\mathbb{P}(|X_{11}| \leq t) \leq C_0 t^\alpha$ holds for all $t > 0$ (it is trivial for $t \geq 1$ since $\mathbb{P}(|X_{11}| \leq t) \leq 1$). Fix i . Write

$$m_i - \left(c_\star - \frac{1}{2} \log n \right) = \frac{1}{n} \sum_{k=1}^n Y_{ik}, \quad Y_{ik} := \log |a_{ik}| - \mathbb{E} \log |a_{ik}| = \log |X_{ik}| - \mathbb{E} \log |X_{ik}|. \quad (\text{B.50})$$

Thus $\{Y_{ik}\}_{k=1}^n$ are i.i.d. mean-zero. We claim $Y := \log |X| - \mathbb{E} \log |X|$ is *subexponential*, i.e. $\|Y\|_{\psi_1} \leq K$ for some $K < \infty$ depending only on the entry law.

Indeed, by sub-Gaussianity of X , for the *right tail* and $t \geq 0$,

$$\mathbb{P}(Y \geq t) = \mathbb{P}(|X| \geq e^{t + \mathbb{E} \log |X|}) \leq 2 \exp(-c e^{2t}), \quad (\text{B.51})$$

which is super-exponential in t . For the *left tail*, the small-ball bound gives, for $t \geq 0$,

$$\mathbb{P}(Y \leq -t) = \mathbb{P}(|X| \leq e^{-t + \mathbb{E} \log |X|}) \leq C_0 e^{\alpha \mathbb{E} \log |X|} e^{-\alpha t} =: \tilde{C}_0 e^{-\alpha t}. \quad (\text{B.52})$$

Hence $\mathbb{P}(|Y| \geq t) \leq Ae^{-Bt}$ for some $A, B > 0$, which implies Y is subexponential (see, e.g., [30, Sec. 2.7–2.8]). Applying Theorem B.1, for all $u > 0$,

$$\mathbb{P}\left(\left|\frac{1}{n} \sum_{k=1}^n Y_{ik}\right| > u\right) \leq 2 \exp\left(-c'n \min\left(\frac{u^2}{K^2}, \frac{u}{K}\right)\right). \quad (\text{B.53})$$

Choose $u = C_1 \sqrt{\frac{\log n}{n}}$ with C_1 large so the RHS is $\leq 2n^{-12}$. A union bound over $i = 1, \dots, n$ yields

$$\mathbb{P}\left(\max_i \left|m_i - \left(c_\star - \frac{1}{2} \log n\right)\right| > C_1 \sqrt{\frac{\log n}{n}}\right) \leq 2n^{-11}. \quad (\text{B.54})$$

The column bound is identical. For the grand mean,

$$\bar{m} - \left(c_\star - \frac{1}{2} \log n\right) = \frac{1}{n^2} \sum_{i,j=1}^n Y_{ij}, \quad (\text{B.55})$$

and the same Bernstein bound with n^2 samples gives a stronger tail; we keep the displayed order for uniformity. Adjusting constants and n large ensures the stated $1 - Cn^{-10}$ bound. \square

Remark B.2. If X_{ij} are standard real Gaussian $\mathcal{N}(0, 1)$ then $c_\star = \mathbb{E} \log |X_{11}| = c_{\beta=1}$. If X_{ij} are standard circular complex Gaussian $\mathcal{CN}(0, 1)$ (with $\mathbb{E}|X_{11}|^2 = 1$) then $c_\star = \mathbb{E} \log |X_{11}| = c_{\beta=2}$, as computed in Lemma B.12.

Lemma B.12. Let $G_1 \sim \mathcal{N}(0, 1)$ and let $G_2 \sim \mathcal{CN}(0, 1)$ where $\mathcal{CN}(0, 1)$ denotes the standard circular complex normal, i.e. $G_2 = X + iY$ with $X, Y \stackrel{\text{i.i.d.}}{\sim} \mathcal{N}(0, \frac{1}{2})$ (equivalently $\mathbb{E}|G_2|^2 = 1$). Then

$$c_{\beta=1} := \mathbb{E} \log |G_1| = -\frac{1}{2}(\gamma + \log 2), \quad c_{\beta=2} := \mathbb{E} \log |G_2| = -\frac{1}{2}\gamma, \quad (\text{B.56})$$

where γ is the Euler-Mascheroni constant. Numerically, $c_{\beta=1} \approx -0.6351814227$ and $c_{\beta=2} \approx -0.2886078324$.

Proof. Let Γ be the gamma function and let $\psi(z) := \Gamma'(z)/\Gamma(z)$ denote the digamma function. Let $Y \sim \text{Gamma}(\alpha, \theta)$ with shape $\alpha > 0$ and scale $\theta > 0$, i.e. with density

$$f_Y(y) = \frac{1}{\Gamma(\alpha)\theta^\alpha} y^{\alpha-1} e^{-y/\theta} \mathbf{1}_{y>0}. \quad (\text{B.57})$$

Then

$$\mathbb{E} \log Y = \int_0^\infty (\log y) f_Y(y) dy. \quad (\text{B.58})$$

Substituting $y = \theta t$ gives

$$\mathbb{E} \log Y = \log \theta + \frac{1}{\Gamma(\alpha)} \int_0^\infty t^{\alpha-1} e^{-t} \log t dt = \log \theta + \frac{\Gamma'(\alpha)}{\Gamma(\alpha)} = \log \theta + \psi(\alpha). \quad (\text{B.59})$$

where we used $\Gamma(\alpha) = \int_0^\infty t^{\alpha-1} e^{-t} dt$ and (for $\alpha > 0$) differentiation under the integral sign, justified by dominated convergence, to obtain $\Gamma'(\alpha) = \int_0^\infty t^{\alpha-1} e^{-t} \log t dt$. For $G_1 \sim \mathcal{N}(0, 1)$, the change of variables $V := G_1^2$ gives the density

$$f_V(v) = \frac{1}{\sqrt{2\pi v}} e^{-v/2} \mathbf{1}_{v>0}, \quad (\text{B.60})$$

which is $\text{Gamma}(\frac{1}{2}, 2)$ (shape $\frac{1}{2}$, scale 2). Hence

$$\mathbb{E} \log |G_1| = \frac{1}{2} \mathbb{E} \log(G_1^2) = \frac{1}{2} (\psi(\frac{1}{2}) + \log 2). \quad (\text{B.61})$$

For $G_2 = X + iY$ with $X, Y \stackrel{\text{i.i.d.}}{\sim} \mathcal{N}(0, \frac{1}{2})$, write $X = \frac{X_0}{\sqrt{2}}$ and $Y = \frac{Y_0}{\sqrt{2}}$ with $X_0, Y_0 \stackrel{\text{i.i.d.}}{\sim} \mathcal{N}(0, 1)$. Then

$$|G_2|^2 = X^2 + Y^2 = \frac{X_0^2 + Y_0^2}{2}. \quad (\text{B.62})$$

Since $S := X_0^2 + Y_0^2$ has density $f_S(s) = \frac{1}{2} e^{-s/2} \mathbf{1}_{s>0}$ (i.e. $\chi_2^2 = \text{Gamma}(1, 2)$), it follows that $|G_2|^2$ has density $e^{-u} \mathbf{1}_{u>0}$, i.e. $|G_2|^2 \sim \text{Gamma}(1, 1)$. Therefore

$$\mathbb{E} \log |G_2| = \frac{1}{2} \mathbb{E} \log(|G_2|^2) = \frac{1}{2} \psi(1). \quad (\text{B.63})$$

Using $\psi(1) = -\gamma$ and $\psi(\frac{1}{2}) = -\gamma - 2 \log 2$ [66, §5.4(ii), Eqns. (5.4.12)-(5.4.13)] gives $c_{\beta=1} = -\frac{1}{2}(\gamma + \log 2)$ and $c_{\beta=2} = -\frac{1}{2}\gamma$. The numerical values follow from $\gamma \approx 0.5772156649$ [66, §5.2(ii), Eq. (5.2.3)]. \square

Lemma B.13. *Let $A_n = (a_{ij})$ be Wigner- β (GOE/GUE) with the $1/\sqrt{n}$ scaling and set $r_i := \|A_n(i, :)\|_2$ and $c_j := \|A_n(:, j)\|_2$. Then there exists $C > 0$ such that, with probability at least $1 - Cn^{-10}$,*

$$\max_i |r_i - 1| \leq C \sqrt{\frac{\log n}{n}}, \quad \max_j |c_j - 1| \leq C \sqrt{\frac{\log n}{n}}. \quad (\text{B.64})$$

Proof. We prove the row bound; the column bound is identical by symmetry. Fix $i \in \{1, \dots, n\}$ and write

$$r_i^2 = \sum_{k=1}^n |a_{ik}|^2 = \sum_{k \neq i} |a_{ik}|^2 + |a_{ii}|^2. \quad (\text{B.65})$$

For Wigner- β under the $1/\sqrt{n}$ scaling, the off-diagonals $\{a_{ik} : k \neq i\}$ are independent, mean zero, with $\mathbb{E}|a_{ik}|^2 = 1/n$; the diagonal has $\mathbb{E}|a_{ii}|^2 = \nu_\beta/n$ with $\nu_\beta = 2$ in GOE and $\nu_\beta = 1$ in GUE. Hence

$$\mathbb{E} r_i^2 = \frac{n-1}{n} + \frac{\nu_\beta}{n} = \begin{cases} 1 + \frac{1}{n}, & \beta = 1 \text{ (GOE)}, \\ 1, & \beta = 2 \text{ (GUE)}. \end{cases} \quad (\text{B.66})$$

Define centered variables $Y_{ik} := |a_{ik}|^2 - \mathbb{E}|a_{ik}|^2$ for $k \neq i$ and $X_{ii} := |a_{ii}|^2 - \mathbb{E}|a_{ii}|^2$. Since a_{ik} is sub-Gaussian with $\|a_{ik}\|_{\psi_2} = O(n^{-1/2})$, Vershynin's inequality [30, Lem. 2.7.4] gives $\|Y_{ik}\|_{\psi_1} = O(n^{-1})$ uniformly in $k \neq i$ (and in β), and similarly $\|X_{ii}\|_{\psi_1} = O(n^{-1})$.

Therefore, applying Bernstein's inequality Theorem B.1 to the n independent mean-zero variables $\{Y_{ik} : k \neq i\} \cup \{X_{ii}\}$ yields, for $u \in (0, 1)$,

$$\mathbb{P}\left(|r_i^2 - \mathbb{E}r_i^2| > u\right) \leq 2 \exp(-cn u^2), \quad (\text{B.67})$$

for some constant $c > 0$. Choose $u := C_0 \sqrt{(\log n)/n}$ with C_0 large enough so that the RHS is $\leq n^{-11}$. On the event $\{|r_i^2 - \mathbb{E}r_i^2| \leq u\}$ we get

$$\left|r_i - \sqrt{\mathbb{E}r_i^2}\right| = \frac{|r_i^2 - \mathbb{E}r_i^2|}{r_i + \sqrt{\mathbb{E}r_i^2}} \leq \frac{|r_i^2 - \mathbb{E}r_i^2|}{\sqrt{\mathbb{E}r_i^2}} \leq |r_i^2 - \mathbb{E}r_i^2| \leq u. \quad (\text{B.68})$$

Hence

$$|r_i - 1| \leq |r_i - \sqrt{\mathbb{E}r_i^2}| + |\sqrt{\mathbb{E}r_i^2} - 1| \leq u + |\mathbb{E}r_i^2 - 1| \leq C_0 \sqrt{\frac{\log n}{n}} + \frac{\mathbf{1}_{\{\beta=1\}}}{n}. \quad (\text{B.69})$$

Absorb the negligible $1/n$ term into the $\sqrt{(\log n)/n}$ term by increasing C_0 if needed, to obtain

$$\mathbb{P}\left(|r_i - 1| > C_1 \sqrt{\frac{\log n}{n}}\right) \leq n^{-11}. \quad (\text{B.70})$$

A union bound over $i = 1, \dots, n$ yields

$$\mathbb{P}\left(\max_i |r_i - 1| > C \sqrt{\frac{\log n}{n}}\right) \leq C n^{-10} \quad (\text{B.71})$$

for an adjusted constant $C > 0$, proving the first part of Eq. (B.64). The column bound follows identically by applying the same argument to $\{a_{ki}\}_k$. \square

Lemma B.14. *Let $A_n = (a_{ij})$ be Wigner- β with the $1/\sqrt{n}$ scaling, and define the row-/column/grand log-means*

$$m_i := \frac{1}{n} \sum_{k=1}^n \log |a_{ik}|, \quad n_j := \frac{1}{n} \sum_{k=1}^n \log |a_{kj}|, \quad \bar{m} := \frac{1}{n^2} \sum_{i,k=1}^n \log |a_{ik}|. \quad (\text{B.72})$$

Let c_β as in Lemma B.12. Then $\max_i |m_i - (c_\beta - \frac{1}{2} \log n)| = O_{\text{a.s.}}(\sqrt{(\log n)/n})$, and similarly for n_j and \bar{m} .

Proof. We give the row bound; the column bound is the same, and the grand average follows similarly. Set $\mu := c_\beta - \frac{1}{2} \log n$. Fix i and split

$$m_i - \mu = \frac{1}{n} \sum_{k \neq i} (\log |a_{ik}| - \mu) + \underbrace{\left(\frac{1}{n} \log |a_{ii}| - \frac{\mu}{n}\right)}_{:= \Delta_i}. \quad (\text{B.73})$$

For $k \neq i$ we have $a_{ik} \xrightarrow{d} g_\beta/\sqrt{n}$, so, taking $Y_{ik} := \log |a_{ik}|$ where $k \neq i$, we get $\mathbb{E}Y_{ik} = \mathbb{E} \log |g_\beta| - \frac{1}{2} \log n = c_\beta - \frac{1}{2} \log n = \mu$. The variables $\{Y_{ik}\}_{k \neq i}$ are independent. Set

$$W_{ik} := Y_{ik} - \mu = \log |a_{ik}| - \left(c_\beta - \frac{1}{2} \log n\right), \quad k \neq i. \quad (\text{B.74})$$

Following the steps of Lemma B.11, each W_{ik} is centered sub-exponential with parameters independent of n and k . Therefore, for any $u \in (0, 1)$,

$$\mathbb{P}\left(\left|\frac{1}{n} \sum_{k \neq i} W_{ik}\right| > u\right) \leq 2 \exp(-cn u^2), \quad (\text{B.75})$$

for some absolute $c > 0$ (depending only on β). It remains to control the diagonal contribution Δ_i ,

$$\Delta_i = \frac{1}{n} \log |a_{ii}| - \frac{1}{n} \left(c_\beta - \frac{1}{2} \log n \right). \quad (\text{B.76})$$

Since $a_{ii} \stackrel{d}{=} \sqrt{\nu_\beta} g_1 / \sqrt{n}$ with $\nu_\beta = 2$ for GOE and $\nu_\beta = 1$ for GUE,

$$\mathbb{E} \log |a_{ii}| = \mathbb{E} \log |\sqrt{\nu_\beta} g_1| - \frac{1}{2} \log n = \left(\mathbb{E} \log |g_1| + \frac{1}{2} \log \nu_\beta \right) - \frac{1}{2} \log n. \quad (\text{B.77})$$

Thus $\mathbb{E} \Delta_i = \frac{1}{n} \left(\mathbb{E} \log |g_1| - c_\beta + \frac{1}{2} \log \nu_\beta \right) = O(1/n)$, and Δ_i itself is sub-exponential with scale $O(1/n)$ (being n^{-1} times a sub-exponential variable). In particular, for $u \in (0, 1)$,

$$\mathbb{P}(|\Delta_i - \mathbb{E} \Delta_i| > u/3) \leq 2 \exp(-c' n u) \leq 2 \exp(-c' n u^2), \quad (\text{B.78})$$

for some $c' > 0$ (the last inequality since $u \in (0, 1)$). Moreover, $|\mathbb{E} \Delta_i| = \frac{1}{n} |\mathbb{E} \log |a_{ii}| - \mu| = O(1/n) \leq u/3$ for all large n when $u = K \sqrt{(\log n)/n}$. Combining Eq. (B.75) and Eq. (B.78) by a union bound gives

$$\mathbb{P}\left(|m_i - (c_\beta - \frac{1}{2} \log n)| > u\right) \leq C_1 \exp(-c_1 n u^2). \quad (\text{B.79})$$

A union bound over $i = 1, \dots, n$ yields the result. The case for n_j is identical. For the grand mean, decompose

$$\bar{m} = \frac{1}{n^2} \sum_{i \neq k} \log |a_{ik}| + \frac{1}{n^2} \sum_{i=1}^n \log |a_{ii}| = \frac{2}{n^2} \sum_{1 \leq i < k \leq n} \log |a_{ik}| + \frac{1}{n^2} \sum_{i=1}^n \log |a_{ii}|. \quad (\text{B.80})$$

The variables $\{\log |a_{ik}|\}_{i < k}$ are independent and identically distributed with mean $c_\beta - \frac{1}{2} \log n$ and are subexponential (as in Lemma B.11). Applying Theorem B.1 to the sum over $i < k$ gives a tail bound of the form $\mathbb{P}(|\cdot| > u) \leq 2 \exp(-cn u^2)$ for $u \in (0, 1)$. The diagonal term is $\frac{1}{n^2} \sum_{i=1}^n \log |a_{ii}|$, which has $O((\log n)/n)$ magnitude in expectation and subexponential fluctuations of scale $O(1/n)$, hence is negligible at the level $u_n := K \sqrt{(\log n)/n}$. Summing the resulting bounds over n and applying Borel-Cantelli yields the stated almost sure control of \bar{m} . \square

B.2 Proofs of Section 2.4

Proof of Theorem 2.1. Let $r_i := \|A_n(i, :)\|_2$ and $c_j := \|A_n(:, j)\|_2$. Lemma B.6 yields with high probability

$$\max_i |r_i - 1|, \max_j |c_j - 1| \leq C_0 \sqrt{\frac{\log n}{n}}. \quad (\text{B.81})$$

Using Corollary B.7,

$$D_n^L = I + \Delta_n^L, \quad D_n^R = I + \Delta_n^R, \quad \|\Delta_n^L\|_{\mathcal{O}}, \|\Delta_n^R\|_{\mathcal{O}} \leq C_1 \sqrt{\frac{\log n}{n}}. \quad (\text{B.82})$$

For LUI,

$$A_n^L (A_n^L)^\dagger = D_n^L A_n A_n^\dagger D_n^L = A_n A_n^\dagger + E_n^L, \quad (\text{B.83})$$

with $E_n^L := \Delta_n^L A_n A_n^\dagger + A_n A_n^\dagger \Delta_n^L + \Delta_n^L A_n A_n^\dagger \Delta_n^L$. Lemma B.8 gives

$$\|E_n^L\|_{\mathcal{O}} \leq (2\|\Delta_n^L\|_{\mathcal{O}} + \|\Delta_n^L\|_{\mathcal{O}}^2) \|A_n\|_{\mathcal{O}}^2 \leq C_2 \sqrt{\frac{\log n}{n}} \cdot \|A_n\|_{\mathcal{O}}^2. \quad (\text{B.84})$$

By Theorem B.3 (with $p = n$, $\sigma^2 = 1$) we have

$$\lambda_{\max}\left(\frac{1}{n} X_n X_n^\dagger\right) \rightarrow 4 \implies \|A_n\|_{\mathcal{O}} = \sqrt{\lambda_{\max}(A_n A_n^\dagger)} \rightarrow 2 \quad (\text{B.85})$$

almost surely. Define the high-probability event

$$\mathcal{E}_n := \left\{ \max_i |r_i - 1| \leq C_0 \sqrt{\frac{\log n}{n}} \right\}. \quad (\text{B.86})$$

By Lemma B.6, $\mathbb{P}(\mathcal{E}_n^c) \leq C n^{-10}$ and hence $\sum_{n=1}^{\infty} \mathbb{P}(\mathcal{E}_n^c) < \infty$; by the Borel–Cantelli lemma, \mathcal{E}_n holds eventually almost surely. So from Eqs. (B.82), (B.84) and (B.85) we get

$$\|E_n^L\|_{\mathcal{O}} \rightarrow 0 \quad \text{almost surely.} \quad (\text{B.87})$$

Now set

$$M_n := A_n A_n^\dagger, \quad N_n := A_n^L (A_n^L)^\dagger, \quad E_n := N_n - M_n = E_n^L. \quad (\text{B.88})$$

For any fixed $z = x + iy$ with $y > 0$, Lemma B.9 gives

$$|m_{N_n}(z) - m_{M_n}(z)| \leq \frac{\|E_n\|_{\mathcal{O}}}{y^2} \xrightarrow[n \rightarrow \infty]{a.s.} 0. \quad (\text{B.89})$$

By Theorem B.2, $m_{M_n}(z) \rightarrow m_{\text{MP}(1,1)}(z)$ almost surely for every such z ; hence we also have $m_{N_n}(z) \rightarrow m_{\text{MP}(1,1)}(z)$ almost surely. Since $\text{MP}(1,1)$ has density $\frac{1}{2\pi x} \sqrt{x(4-x)} \mathbf{1}_{(0,4)}(x)$ on $[0, 4]$, its pushforward under $x \mapsto \sqrt{x}$ has density

$$f(s) = 2s \cdot \frac{1}{2\pi s^2} \sqrt{s^2(4-s^2)} \mathbf{1}_{(0,2)}(s) = \frac{1}{\pi} \sqrt{4-s^2} \mathbf{1}_{[0,2]}(s), \quad (\text{B.90})$$

i.e. the quarter-circle law on $[0, 2]$. By Lemma B.9 the empirical spectral distribution (ESD) of N_n converges almost surely to the $\text{MP}(1,1)$ law supported on $[0, 4]$. Finally, by Lemma B.5 the empirical measure of singular values of A_n^L converges almost surely to the quarter-circle law on $[0, 2]$ with density $f(s) = \frac{1}{\pi} \sqrt{4-s^2} \mathbf{1}_{[0,2]}(s)$.

The RUI case is identical (replace D_n^L by D_n^R and use c_j instead of r_i). \square

Proof of Theorem 2.2. Write $a_{ij} := X_{ij}/\sqrt{n}$ (so $A_n = (a_{ij})$) and define the row/column/grand *log-averages*

$$m_i := \frac{1}{n} \sum_{k=1}^n \log |a_{ik}|, \quad n_j := \frac{1}{n} \sum_{k=1}^n \log |a_{kj}|, \quad \bar{m} := \frac{1}{n^2} \sum_{i,j=1}^n \log |a_{ij}|. \quad (\text{B.91})$$

By Proposition B.10 (symmetric scale),

$$\log(D_n^{BL})_{ii} = -m_i + \frac{1}{2}\bar{m}, \quad \log(D_n^{BR})_{jj} = -n_j + \frac{1}{2}\bar{m}. \quad (\text{B.92})$$

Since $\mathbb{P}(X_{11} = 0) = 0$, we have $\mathbb{P}(a_{ij} \neq 0 \ \forall i, j) = 1$ for each fixed n , so Proposition B.10 applies almost surely. Moreover, changing (α, β) within the one-parameter family in Proposition B.10 rescales D^{BL} and D^{BR} inversely and leaves $A_n^B = D_n^{BL} A_n D_n^{BR}$ unchanged; the symmetric scale fixes a unique choice of the pair (D_n^{BL}, D_n^{BR}) . Introduce deviations

$$\delta_i := m_i - \left(c_\star - \frac{1}{2} \log n\right), \quad \epsilon_j := n_j - \left(c_\star - \frac{1}{2} \log n\right), \quad \bar{\delta} := \bar{m} - \left(c_\star - \frac{1}{2} \log n\right), \quad (\text{B.93})$$

so that by Lemma B.11, $\max_i |\delta_i|, \max_j |\epsilon_j|, |\bar{\delta}| \leq C_0 \sqrt{\frac{\log n}{n}}$ on the same high probability event. We get,

$$\log(D_n^{BL})_{ii} = -\left(c_\star - \frac{1}{2} \log n + \delta_i\right) + \frac{1}{2}\left(c_\star - \frac{1}{2} \log n + \bar{\delta}\right) = -\frac{c_\star}{2} + \frac{1}{4} \log n + \left(-\delta_i + \frac{1}{2}\bar{\delta}\right). \quad (\text{B.94})$$

Exponentiating and factoring out $e^{-c_\star/2} n^{1/4}$ gives

$$(D_n^{BL})_{ii} = e^{-c_\star/2} n^{1/4} \exp\left(-\delta_i + \frac{1}{2}\bar{\delta}\right) = e^{-c_\star/2} n^{1/4} (1 + \delta_i^{BL}), \quad (\text{B.95})$$

where we define

$$\delta_i^{BL} := \exp\left(-\delta_i + \frac{1}{2}\bar{\delta}\right) - 1. \quad (\text{B.96})$$

Since $|- \delta_i + \frac{1}{2}\bar{\delta}| \leq C_1 \sqrt{\frac{\log n}{n}}$, the elementary bound

$$|e^x - 1| \leq e^{|x|} - 1 \leq |x|e^{|x|} \quad (x \in \mathbb{R}) \quad (\text{B.97})$$

implies $|\delta_i^{BL}| \leq C_2 \sqrt{\frac{\log n}{n}}$ for all i (uniformly on the high-probability event). Define $\Delta_n^{BL} := \text{diag}(\delta_1^{BL}, \dots, \delta_n^{BL})$ so that

$$D_n^{BL} = e^{-c_\star/2} n^{1/4} (I + \Delta_n^{BL}), \quad \|\Delta_n^{BL}\|_{\mathcal{O}} = \max_i |\delta_i^{BL}| \leq C_2 \sqrt{\frac{\log n}{n}}. \quad (\text{B.98})$$

An identical computation (with n_j, ϵ_j) yields

$$D_n^{BR} = e^{-c_\star/2} n^{1/4} (I + \Delta_n^{BR}), \quad \|\Delta_n^{BR}\|_{\mathcal{O}} \leq C_3 \sqrt{\frac{\log n}{n}}. \quad (\text{B.99})$$

Multiplying out with A_n gives the core factorisation. Set, for brevity,

$$\delta_n := C \sqrt{\frac{\log n}{n}} \quad \text{so that} \quad \|I + \Delta_n^{BL}\|_{\mathcal{O}}, \|I + \Delta_n^{BR}\|_{\mathcal{O}} \leq 1 + \delta_n. \quad (\text{B.100})$$

Then for the upper bound

$$\|A_n^B\|_{\mathcal{O}} \leq e^{-c_\star} \sqrt{n} \|I + \Delta_n^{BL}\|_{\mathcal{O}} \|A_n\|_{\mathcal{O}} \|I + \Delta_n^{BR}\|_{\mathcal{O}} \leq e^{-c_\star} \sqrt{n} (1 + \delta_n)^2 \|A_n\|_{\mathcal{O}}. \quad (\text{B.101})$$

By Theorem B.3, $\|A_n\|_{\mathcal{O}} \rightarrow 2$ almost surely; enlarging the constant in δ_n if needed yields

$$\|A_n^B\|_{\mathcal{O}} \leq 2e^{-c_\star} \sqrt{n} (1 + \delta_n) \quad (\text{B.102})$$

for all large n on the same event. For the lower bound, using

$$(I + \Delta_n^{B_L})A_n(I + \Delta_n^{B_R}) = A_n + \Delta_n^{B_L}A_n + A_n\Delta_n^{B_R} + \Delta_n^{B_L}A_n\Delta_n^{B_R}, \quad (\text{B.103})$$

we obtain

$$\begin{aligned} \|(I + \Delta_n^{B_L})A_n(I + \Delta_n^{B_R})\|_{\mathcal{O}} &\geq \|A_n\|_{\mathcal{O}} - \|A_n\|_{\mathcal{O}}(\|\Delta_n^{B_L}\|_{\mathcal{O}} + \|\Delta_n^{B_R}\|_{\mathcal{O}}) \\ &\quad - \|A_n\|_{\mathcal{O}}\|\Delta_n^{B_L}\|_{\mathcal{O}}\|\Delta_n^{B_R}\|_{\mathcal{O}}. \end{aligned} \quad (\text{B.104})$$

On the high-probability event,

$$\|A_n^B\|_{\mathcal{O}} \geq e^{-c_*}\sqrt{n}\|A_n\|_{\mathcal{O}}\left(1 - 2\delta_n - \delta_n^2\right) = 2e^{-c_*}\sqrt{n}(1 - o(1)), \quad (\text{B.105})$$

since $\|A_n\|_{\mathcal{O}} \rightarrow 2$ and $\delta_n \rightarrow 0$. Together with the upper bound,

$$\frac{\|A_n^B\|_{\mathcal{O}}}{\sqrt{n}} \longrightarrow 2e^{-c_*} \quad \text{almost surely.} \quad (\text{B.106})$$

For the normalised matrices $T_n := n^{-1/2}A_n^B$, rewrite as

$$T_n = e^{-c_*}(I + \Delta_n^{B_L})A_n(I + \Delta_n^{B_R}). \quad (\text{B.107})$$

Set

$$H_n := T_n T_n^\dagger, \quad \hat{H}_n := e^{-2c_*}A_n A_n^\dagger. \quad (\text{B.108})$$

Set

$$P_n := A_n(I + \Delta_n^{B_R}), \quad \tilde{H}_n := e^{-2c_*}P_n P_n^\dagger, \quad (\text{B.109})$$

so that

$$H_n = e^{-2c_*}(I + \Delta_n^{B_L})P_n P_n^\dagger(I + \Delta_n^{B_L}). \quad (\text{B.110})$$

Applying Lemma B.8 with $D = I + \Delta_n^{B_L}$ and $A = P_n$ gives

$$\|H_n - \tilde{H}_n\|_{\mathcal{O}} \leq e^{-2c_*}(2\|\Delta_n^{B_L}\|_{\mathcal{O}} + \|\Delta_n^{B_L}\|_{\mathcal{O}}^2)\|P_n\|_{\mathcal{O}}^2. \quad (\text{B.111})$$

Next,

$$\tilde{H}_n - \hat{H}_n = e^{-2c_*}\left(P_n P_n^\dagger - A_n A_n^\dagger\right) = e^{-2c_*}A_n\left((I + \Delta_n^{B_R})(I + \Delta_n^{B_R})^\dagger - I\right)A_n^\dagger, \quad (\text{B.112})$$

hence

$$\|\tilde{H}_n - \hat{H}_n\|_{\mathcal{O}} \leq e^{-2c_*}(\|\Delta_n^{B_R} + (\Delta_n^{B_R})^\dagger\|_{\mathcal{O}} + \|\Delta_n^{B_R}\|_{\mathcal{O}}^2)\|A_n\|_{\mathcal{O}}^2. \quad (\text{B.113})$$

Finally, $\|P_n\|_{\mathcal{O}} \leq \|A_n\|_{\mathcal{O}}\|I + \Delta_n^{B_R}\|_{\mathcal{O}}$, so combining the last two displays yields

$$\|H_n - \hat{H}_n\|_{\mathcal{O}} \leq e^{-2c_*}C(\|\Delta_n^{B_L}\|_{\mathcal{O}} + \|\Delta_n^{B_R}\|_{\mathcal{O}})\|A_n\|_{\mathcal{O}}^2 \quad (\text{B.114})$$

for all large n on the same event (absorbing quadratic terms into the constant C since $\|\Delta\|_{\mathcal{O}} = o(1)$).

On the high-probability event, Eqs. (B.85), (B.98) and (B.99) give

$$\|H_n - \hat{H}_n\|_{\mathcal{O}} = O\left(\sqrt{\frac{\log n}{n}}\right) \xrightarrow[n \rightarrow \infty]{} 0 \quad (\text{B.115})$$

on the high-probability event. By Lemma B.9, $\text{ESD}(H_n)$ and $\text{ESD}(\widehat{H}_n)$ have the same limiting law. By Theorem B.2, $\text{ESD}(A_n A_n^\dagger) \Rightarrow \text{MP}(1, 1)$; therefore $\text{ESD}(\widehat{H}_n) \Rightarrow \text{MP}(1, 1)$ scaled by e^{-2c_\star} . Finally, by Lemma B.5, the empirical measures of the singular values of T_n converge almost surely to the quarter-circle law on $[0, 2e^{-c_\star}]$. The failure probabilities are $\leq Cn^{-10}$; hence $\sum_n \mathbb{P}(\text{fail at } n) < \infty$. By the Borel–Cantelli lemma, the high-probability event (and therefore $\|\Delta_n^{\text{BL}}\|_{\mathcal{O}}, \|\Delta_n^{\text{BR}}\|_{\mathcal{O}} \rightarrow 0$) holds eventually almost surely, which promotes the convergence above to almost sure convergence. \square

Proof of Theorem 2.3. Write $r_i := \|A_n(i, :)\|_2$ and $c_j := \|A_n(:, j)\|_2$, and define $D_n^{\text{L}} := \text{Diag}(1/r_1, \dots, 1/r_n)$, $D_n^{\text{R}} := \text{Diag}(1/c_1, \dots, 1/c_n)$ so that $A_n^{\text{L}} = D_n^{\text{L}} A_n$ and $A_n^{\text{R}} = A_n D_n^{\text{R}}$. Let $\delta_n^{\text{L}} := \max_i |r_i - 1|$ and $\delta_n^{\text{R}} := \max_j |c_j - 1|$. Then

$$\|D_n^{\text{L}} - I\|_{\mathcal{O}} = \max_i \left| \frac{1}{r_i} - 1 \right| = \max_i \frac{|1 - r_i|}{r_i} \leq \frac{\delta_n^{\text{L}}}{\min_i r_i}, \quad \|D_n^{\text{R}} - I\|_{\mathcal{O}} \leq \frac{\delta_n^{\text{R}}}{\min_j c_j}. \quad (\text{B.116})$$

By Lemma B.13, for each n we have $\mathbb{P}(\delta_n^{\text{L}} > \frac{1}{2} \text{ or } \delta_n^{\text{R}} > \frac{1}{2}) \leq Cn^{-10}$. Since $\sum_n Cn^{-10} < \infty$, the Borel–Cantelli lemma implies that $\delta_n^{\text{L}}, \delta_n^{\text{R}} \leq \frac{1}{2}$ for all sufficiently large n almost surely; hence $\min_i r_i, \min_j c_j \geq 1 - \frac{1}{2} = \frac{1}{2}$ and therefore

$$\|D_n^{\text{L}} - I\|_{\mathcal{O}} \leq 2\delta_n^{\text{L}}, \quad \|D_n^{\text{R}} - I\|_{\mathcal{O}} \leq 2\delta_n^{\text{R}} = O\left(\sqrt{\frac{\log n}{n}}\right). \quad (\text{B.117})$$

By Borel–Cantelli this holds almost surely eventually. Set $\Delta_n^{\text{L}} := D_n^{\text{L}} - I$ and $\Delta_n^{\text{R}} := D_n^{\text{R}} - I$. Consider

$$M_n := (A_n^{\text{L}})(A_n^{\text{L}})^\dagger = D_n^{\text{L}} A_n A_n^\dagger D_n^{\text{L}}, \quad N_n := A_n A_n^\dagger. \quad (\text{B.118})$$

By Lemma B.8,

$$\|M_n - N_n\|_{\mathcal{O}} \leq (2\|\Delta_n^{\text{L}}\|_{\mathcal{O}} + \|\Delta_n^{\text{L}}\|_{\mathcal{O}}^2) \|N_n\|_{\mathcal{O}}. \quad (\text{B.119})$$

Theorem B.4 implies $\|A_n\|_{\mathcal{O}} \rightarrow 2$ almost surely, hence $\|N_n\|_{\mathcal{O}} = \|A_n\|_{\mathcal{O}}^2 \rightarrow 4$. Therefore $\|M_n - N_n\|_{\mathcal{O}} \rightarrow 0$ almost surely. By Lemma B.9 M_n and N_n have the same limiting ESD. Since the non-zero eigenvalues of N_n (resp. M_n) are the squares of the singular values of A_n (resp. A_n^{L}), the singular-value ESDs of A_n^{L} and A_n have the same limit. Finally, by Theorem B.4, the eigenvalue ESD of A_n converges to semicircle on $[-2, 2]$, hence its singular-value ESD converges to the quarter-circle on $[0, 2]$ (pushforward by $x \mapsto |x|$; Lemma B.5). The right-balanced case A_n^{R} is identical, replacing D_n^{L} by D_n^{R} . \square

Proof of Theorem 2.4. Let $a_{ij} = (A_n)_{ij}$ and define the row/column/grand log-means

$$m_i := \frac{1}{n} \sum_{k=1}^n \log |a_{ik}|, \quad n_j := \frac{1}{n} \sum_{k=1}^n \log |a_{kj}|, \quad \bar{m} := \frac{1}{n^2} \sum_{i,j=1}^n \log |a_{ij}|. \quad (\text{B.120})$$

By Proposition B.10 (symmetric scale),

$$\log(D_n^{\text{BL}})_{ii} = -m_i + \frac{1}{2}\bar{m}, \quad \log(D_n^{\text{BR}})_{jj} = -n_j + \frac{1}{2}\bar{m}. \quad (\text{B.121})$$

By Lemma B.14,

$$\max_i \left| m_i - \left(c_\beta - \frac{1}{2} \log n \right) \right|, \quad \max_j \left| n_j - \left(c_\beta - \frac{1}{2} \log n \right) \right|, \quad \left| \bar{m} - \left(c_\beta - \frac{1}{2} \log n \right) \right| = O_{\text{a.s.}}\left(\sqrt{\frac{\log n}{n}}\right). \quad (\text{B.122})$$

Define deviations $\delta_i, \epsilon_j, \bar{\delta}$ exactly as in *Proof of Theorem 2.2* with c_\star replaced by c_β . Then the same computation as in *Proof of Theorem 2.2* yields diagonal matrices $\Delta_n^{\text{BL}}, \Delta_n^{\text{BR}}$ such that

$$D_n^{\text{BL}} = e^{-c_\beta/2} n^{1/4} (I + \Delta_n^{\text{BL}}), \quad D_n^{\text{BR}} = e^{-c_\beta/2} n^{1/4} (I + \Delta_n^{\text{BR}}), \quad (\text{B.123})$$

with

$$\|\Delta_n^{\text{BL}}\|_{\mathcal{O}} + \|\Delta_n^{\text{BR}}\|_{\mathcal{O}} = O_{\text{a.s.}}\left(\sqrt{\frac{\log n}{n}}\right). \quad (\text{B.124})$$

In particular, $\|\Delta_n^{\text{BL}}\|_{\mathcal{O}}, \|\Delta_n^{\text{BR}}\|_{\mathcal{O}} \rightarrow 0$ almost surely.

Set $T_n := n^{-1/2} A_n^{\text{B}}$. Using Eq. (B.123),

$$T_n = e^{-c_\beta} (I + \Delta_n^{\text{BL}}) A_n (I + \Delta_n^{\text{BR}}). \quad (\text{B.125})$$

Define

$$H_n := T_n T_n^\dagger, \quad \hat{H}_n := e^{-2c_\beta} A_n^2. \quad (\text{B.126})$$

(Since A_n is Hermitian, $A_n A_n^\dagger = A_n^2$.) Set

$$P_n := A_n (I + \Delta_n^{\text{BR}}), \quad \tilde{H}_n := e^{-2c_\beta} P_n P_n^\dagger. \quad (\text{B.127})$$

Then $H_n = e^{-2c_\beta} (I + \Delta_n^{\text{BL}}) P_n P_n^\dagger (I + \Delta_n^{\text{BL}})$, and applying Lemma B.8 with $D = I + \Delta_n^{\text{BL}}$ and $A = P_n$ gives

$$\|H_n - \tilde{H}_n\|_{\mathcal{O}} \leq e^{-2c_\beta} (2\|\Delta_n^{\text{BL}}\|_{\mathcal{O}} + \|\Delta_n^{\text{BL}}\|_{\mathcal{O}}^2) \|P_n\|_{\mathcal{O}}^2. \quad (\text{B.128})$$

Next,

$$\tilde{H}_n - \hat{H}_n = e^{-2c_\beta} \left(P_n P_n^\dagger - A_n^2 \right) = e^{-2c_\beta} A_n \left((I + \Delta_n^{\text{BR}})(I + \Delta_n^{\text{BR}})^\dagger - I \right) A_n, \quad (\text{B.129})$$

so

$$\|\tilde{H}_n - \hat{H}_n\|_{\mathcal{O}} \leq e^{-2c_\beta} (\|\Delta_n^{\text{BR}} + (\Delta_n^{\text{BR}})^\dagger\|_{\mathcal{O}} + \|\Delta_n^{\text{BR}}\|_{\mathcal{O}}^2) \|A_n\|_{\mathcal{O}}^2. \quad (\text{B.130})$$

Also $\|P_n\|_{\mathcal{O}} \leq \|A_n\|_{\mathcal{O}} \|I + \Delta_n^{\text{BR}}\|_{\mathcal{O}}$. Since Theorem B.4 gives $\|A_n\|_{\mathcal{O}} \rightarrow 2$ almost surely and Eq. (B.124) gives $\|\Delta_n^{\text{BL}}\|_{\mathcal{O}} + \|\Delta_n^{\text{BR}}\|_{\mathcal{O}} \rightarrow 0$ almost surely, combining Eq. (B.128)-Eq. (B.130) yields

$$\|H_n - \hat{H}_n\|_{\mathcal{O}} \xrightarrow[n \rightarrow \infty]{\text{a.s.}} 0. \quad (\text{B.131})$$

By Lemma B.9, $\text{ESD}(H_n)$ and $\text{ESD}(\hat{H}_n)$ have the same limiting law.

By Theorem B.4, the eigenvalue ESD of A_n converges almost surely to the semicircle law on $[-2, 2]$; therefore the eigenvalue ESD of A_n^2 converges almost surely to the pushforward of semicircle under $x \mapsto x^2$, which is $\text{MP}(1, 1)$ on $[0, 4]$. Hence $\text{ESD}(\hat{H}_n)$ converges almost surely to $\text{MP}(1, 1)$ scaled by e^{-2c_β} . Finally, by Lemma B.5, the empirical singular-value measures of T_n converge almost surely to the quarter-circle law on $[0, 2e^{-c_\beta}]$. Moreover, taking operator norms in Eq. (B.125) and using $\|A_n\|_{\mathcal{O}} \rightarrow 2$ and $\|\Delta_n^{\text{BL}}\|_{\mathcal{O}}, \|\Delta_n^{\text{BR}}\|_{\mathcal{O}} \rightarrow 0$ yields

$$\|A_n^{\text{B}}\|_{\mathcal{O}} = 2e^{-c_\beta} \sqrt{n} (1 + o(1)) \quad \text{almost surely,} \quad (\text{B.132})$$

which implies the claimed stretched support. \square

References

- [1] L. Amico, R. Fazio, A. Osterloh and V. Vedral, *Entanglement in many-body systems*, *Rev. Mod. Phys.* **80** (2008) 517–576, [[quant-ph/0703044](#)].
- [2] P. Calabrese, J. Cardy and B. Doyon, *Entanglement entropy in extended quantum systems*, *Journal of Physics A: Mathematical and Theoretical* **42** (dec, 2009) 500301.
- [3] M. Srednicki, *Entropy and area*, *Phys. Rev. Lett.* **71** (1993) 666–669, [[hep-th/9303048](#)].
- [4] C. Holzhey, F. Larsen and F. Wilczek, *Geometric and renormalized entropy in conformal field theory*, *Nucl. Phys. B* **424** (1994) 443–467, [[hep-th/9403108](#)].
- [5] P. Calabrese and J. L. Cardy, *Entanglement entropy and quantum field theory*, *J. Stat. Mech.* **0406** (2004) P06002, [[hep-th/0405152](#)].
- [6] S. Ryu and T. Takayanagi, *Holographic derivation of entanglement entropy from AdS/CFT*, *Phys. Rev. Lett.* **96** (2006) 181602, [[hep-th/0603001](#)].
- [7] T. Takayanagi and K. Umemoto, *Entanglement of purification through holographic duality*, *Nature Phys.* **14** (2018) 573–577, [[1708.09393](#)].
- [8] M. Van Raamsdonk, *Building up spacetime with quantum entanglement*, *Gen. Rel. Grav.* **42** (2010) 2323–2329, [[1005.3035](#)].
- [9] J. M. Maldacena, *The Large N limit of superconformal field theories and supergravity*, *Adv. Theor. Math. Phys.* **2** (1998) 231–252, [[hep-th/9711200](#)].
- [10] T. Takayanagi, *Essay: Emergent Holographic Spacetime from Quantum Information*, *Phys. Rev. Lett.* **134** (2025) 240001, [[2506.06595](#)].
- [11] P. Hosur, X.-L. Qi, D. A. Roberts and B. Yoshida, *Chaos in quantum channels*, *JHEP* **02** (2016) 004, [[1511.04021](#)].
- [12] J. Dubail, *Entanglement scaling of operators: a conformal field theory approach, with a glimpse of simulability of long-time dynamics in $1 + 1d$* , *J. Phys. A* **50** (2017) 234001, [[1612.08630](#)].
- [13] L. Nie, M. Nozaki, S. Ryu and M. T. Tan, *Signature of quantum chaos in operator entanglement in 2d CFTs*, *J. Stat. Mech.* **1909** (2019) 093107, [[1812.00013](#)].
- [14] Y. Nakata, T. Takayanagi, Y. Taki, K. Tamaoka and Z. Wei, *New holographic generalization of entanglement entropy*, *Phys. Rev. D* **103** (2021) 026005, [[2005.13801](#)].
- [15] A. Mollabashi, N. Shiba, T. Takayanagi, K. Tamaoka and Z. Wei, *Aspects of pseudoentropy in field theories*, *Phys. Rev. Res.* **3** (2021) 033254, [[2106.03118](#)].
- [16] A. J. Parzygnat, T. Takayanagi, Y. Taki and Z. Wei, *SVD entanglement entropy*, *JHEP* **12** (2023) 123, [[2307.06531](#)].
- [17] K. Doi, J. Harper, A. Mollabashi, T. Takayanagi and Y. Taki, *Pseudoentropy in dS/CFT and Timelike Entanglement Entropy*, *Phys. Rev. Lett.* **130** (2023) 031601, [[2210.09457](#)].
- [18] K. Doi, J. Harper, A. Mollabashi, T. Takayanagi and Y. Taki, *Timelike entanglement entropy*, *JHEP* **05** (2023) 052, [[2302.11695](#)].
- [19] A. Milekhin, Z. Adamska and J. Preskill, *Observable and computable entanglement in time*, [2502.12240](#).
- [20] Y. Hikida, T. Nishioka, T. Takayanagi and Y. Taki, *CFT duals of three-dimensional de Sitter gravity*, *JHEP* **05** (2022) 129, [[2203.02852](#)].

[21] Y. Hikida, T. Nishioka, T. Takayanagi and Y. Taki, *Holography in de Sitter Space via Chern-Simons Gauge Theory*, *Phys. Rev. Lett.* **129** (2022) 041601, [[2110.03197](#)].

[22] S. Grieninger, K. Ikeda and D. E. Kharzeev, *Temporal entanglement entropy as a probe of renormalization group flow*, *JHEP* **05** (2024) 030, [[2312.08534](#)].

[23] T. Nishioka, T. Takayanagi and Y. Taki, *Topological pseudo entropy*, *JHEP* **09** (2021) 015, [[2107.01797](#)].

[24] P. Caputa, S. Purkayastha, A. Saha and P. Sulkowski, *Musings on SVD and pseudo entanglement entropies*, *JHEP* **11** (2024) 103, [[2408.06791](#)].

[25] P. Caputa, B. Chen, T. Takayanagi and T. Tsuda, *Thermal pseudo-entropy*, *JHEP* **01** (2025) 003, [[2411.08948](#)].

[26] E. Edvardsson, J. L. K. König and M. Stålhammar, *Biorthogonal Renormalization*, [2212.06004](#).

[27] J. Uhlmann, *A generalized matrix inverse that is consistent with respect to diagonal transformations*, *SIAM Journal on Matrix Analysis and Applications* **39** (2018) 781–800.

[28] U. G. Rothblum and S. A. Zenios, *Scalings of matrices satisfying line-product constraints and generalizations*, *Linear Algebra and its Applications* **175** (1992) 159–175.

[29] D. N. Page, *Average entropy of a subsystem*, *Phys. Rev. Lett.* **71** (1993) 1291–1294, [[gr-qc/9305007](#)].

[30] R. Vershynin, *High-Dimensional Probability: An Introduction with Applications in Data Science 1st ed.*, vol. 47 of *Cambridge Series in Statistical and Probabilistic Mathematics*. Cambridge University Press, Cambridge, 2018, [10.1017/9781108231596](#).

[31] F. Mezzadri, *How to generate random matrices from the classical compact groups*, *Notices Am. Math. Soc.* **54** (2007) 592–604, [[math-ph/0609050](#)].

[32] K. Zyczkowski and H.-J. Sommers, *Induced measures in the space of mixed quantum states*, *J. Phys. A* **34** (2001) 7111–7125, [[quant-ph/0012101](#)].

[33] V. Balasubramanian, J. R. Fliss, R. G. Leigh and O. Parrikar, *Multi-boundary entanglement in Chern-Simons theory and link invariants*, *Journal of High Energy Physics* **2017** (apr, 2017) , [[1611.05460](#)].

[34] V. Balasubramanian, M. DeCross, J. Fliss, A. Kar, R. G. Leigh and O. Parrikar, *Entanglement Entropy and the Colored Jones Polynomial*, *JHEP* **05** (2018) 038, [[1801.01131](#)].

[35] A. Dwivedi, S. Dwivedi, B. P. Mandal, P. Ramadevi and V. K. Singh, *Topological entanglement and hyperbolic volume*, *Journal of High Energy Physics* **2021** (2021) 1–37, [[2106.03396](#)].

[36] D. Hall, J.-S. B. Tai, L. H. Kauffman and I. I. Smalyukh, *Fusion and fission of particle-like chiral nematic vortex knots*, *Nature Physics* (Dec., 2025) .

[37] R. G. Leigh and P.-C. Pai, *Complexity for link complement states in Chern-Simons theory*, *Phys. Rev. D* **104** (2021) 065005, [[2101.03443](#)].

[38] K. Habiro, *On the colored Jones polynomial of some simple links*, *RIMS Kokyuroku* **1172** (2000) 34–43.

[39] D. C. Brody, *Biorthogonal quantum mechanics*, *J. Phys. A: Math. Theor.* **47** (2014) 035305.

[40] P.-Y. Chang, J.-S. You, X. Wen and S. Ryu, *Entanglement spectrum and entropy in topological non-Hermitian systems and non-unitary conformal field theories*, *Phys. Rev. Res.* **2** (2020) 033069, [[1909.01346](#)].

[41] Z. Yang, C. Lu and X. Lu, *Entanglement entropy on generalized Brillouin zone*, *Phys. Rev. B* **110** (2024) 235127, [[2406.15564](#)].

[42] L. Herviou, N. Regnault and J. H. Bardarson, *Entanglement spectrum and symmetries in non-Hermitian fermionic non-interacting models*, *SciPost Phys.* **7** (2019) 069, [[1908.09852](#)].

[43] Y.-T. Tu, Y.-C. Tzeng and P.-Y. Chang, *Rényi entropies and negative central charges in non-Hermitian quantum systems*, *SciPost Phys.* **12** (2022) 194, [[2107.13006](#)].

[44] P.-Y. Yang and Y.-C. Tzeng, *Entanglement Hamiltonian and effective temperature of non-Hermitian quantum spin ladders*, *SciPost Phys. Core* **7** (2024) 074, [[2409.17062](#)].

[45] H.-H. Lu and P.-Y. Chang, *Biorthogonal quench dynamics of entanglement and quantum geometry in PT-symmetric non-Hermitian systems*, [2507.20155](#).

[46] Z. Chen, R. Meyer and Z.-Y. Xian, *Entropy Measures for Transition Matrices in Random Systems*, [2508.09261](#).

[47] C. Korff, *Pt symmetry of the non-hermitian xx spin-chain: non-local bulk interaction from complex boundary fields*, *Journal of Physics A: Mathematical and Theoretical* **41** (jun, 2008) 295206.

[48] H. Suzuki, *Transport properties of the XX chain in a staggered magnetic field*, *Bull. Nihon Univ. Sch. Dent.* **44** (2016) 5–16.

[49] S. Schafer-Nameki, A. Tiwari, A. Warman and C. Zhang, *SymTFT Approach for Mixed States with Non-Invertible Symmetries*, [2507.05350](#).

[50] J. Harper, T. Kawamoto, R. Maeda, N. Nakamura and T. Takayanagi, *Non-hermitian Density Matrices from Time-like Entanglement and Wormholes*, [2512.13800](#).

[51] W. Roga, Z. Puchała, L. Rudnicki and K. Życzkowski, *Entropic trade-off relations for quantum operations*, *Phys. Rev. A* **87** (Mar, 2013) 032308.

[52] V. Cappellini, H.-J. Sommers, W. Bruzda and K. Życzkowski, *Random bistochastic matrices*, *Journal of Physics A: Mathematical and Theoretical* **42** (aug, 2009) 365209.

[53] M. Idel, *A review of matrix scaling and sinkhorn’s normal form for matrices and positive maps*, [1609.06349](#).

[54] A. Lucas, *Hydrodynamic transport in strongly coupled disordered quantum field theories*, *New Journal of Physics* **17** (2015) 113007, [[1506.02662](#)].

[55] K. Brandner and U. Seifert, *Multi-terminal thermoelectric transport in a magnetic field: bounds on onsager coefficients and efficiency*, *New Journal of Physics* **15** (2013) 105003, [[1308.2179](#)].

[56] P. Jacquod, R. S. Whitney, J. Meair and M. Büttiker, *Onsager relations in coupled electric, thermoelectric, and spin transport: The tenfold way*, *Physical Review B* **86** (2012) 155118, [[1207.1629](#)].

[57] A. Lucas, R. A. Davison and S. Sachdev, *Hydrodynamic theory of thermoelectric transport and negative magnetoresistance in weyl semimetals*, *Proceedings of the National Academy of Sciences* **113** (2016) 9463, [[1604.08598](#)].

- [58] M. A. Levin and X.-G. Wen, *String-net condensation: A physical mechanism for topological phases*, [cond-mat/0404617](https://arxiv.org/abs/0404617).
- [59] T. Lan and X.-G. Wen, *Topological quasiparticles and the holographic bulk-edge relation in 2+1d string-net models*, [1311.1784](https://arxiv.org/abs/1311.1784).
- [60] A. Francuz, L. Lootens, F. Verstraete and J. Dziarmaga, *Variational methods for characterizing matrix product operator symmetries*, [Physical Review B **104** \(2021\) 195152](https://doi.org/10.1103/PhysRevB.104.195152), [\[2107.05265\]](https://arxiv.org/abs/2107.05265).
- [61] W. Detmold and M. G. Endres, *Signal/noise optimization strategies for stochastically estimated correlation functions*, in *Proceedings of Science (LATTICE2014)*, p. 170, 2015. [1409.5667](https://arxiv.org/abs/1409.5667).
- [62] B. Blossier, M. Della Morte, G. von Hippel, T. Mendes and R. Sommer, *On the generalized eigenvalue method for energies and matrix elements in lattice field theory*, [0902.1265](https://arxiv.org/abs/0902.1265).
- [63] O. M. Smirnov, *Revisiting the radio interferometer measurement equation. ii. calibration and direction-dependent effects*, [Astronomy & Astrophysics **527** \(2011\) A106](https://doi.org/10.1007/s00159-011-0106-6), [\[1101.1765\]](https://arxiv.org/abs/1101.1765).
- [64] Z. Bai and J. W. Silverstein, *Spectral Analysis of Large Dimensional Random Matrices*. Springer Series in Statistics. Springer, New York, NY, 2 ed., 2010, [10.1007/978-1-4419-0661-8](https://doi.org/10.1007/978-1-4419-0661-8).
- [65] T. Tao, *Topics in Random Matrix Theory*, vol. 132 of *Graduate Studies in Mathematics*. American Mathematical Society, Providence, RI, 2012, [10.1090/gsm/132](https://doi.org/10.1090/gsm/132).
- [66] “NIST Digital Library of Mathematical Functions.” <https://dlmf.nist.gov/>, Release 1.2.5 of 2025-12-15 (accessed 2025-12-23).